Department of Physics and Astronomy

Heidelberg University

Bachelor Thesis in Physics

submitted by

Torben Marinus Leeflang

born in Flörsheim am Main (Germany)

2023

Background study of inelastic neutrino interactions for the SHADOWS proton beam dump experiment

This Bachelor Thesis has been carried out by Torben Marinus Leeflang at the
Kirchhoff-Institut für Physik Institute in Heidelberg
under the supervision of
Prof. Dr. Hans–Christian Schultz–Coulon

Abstract

This thesis covers the analysis of background originating from inelastic neutrino interactions using Monte Carlo simulations for a new proton beam dump experiment called SHADOWS (Search for Hidden And Dark Objects With the SPS). The aim of the experiment is to find Feebly-Interacting Particles (FIPs). Some of these particles could potentially provide experimental evidence for multiple important theories and could serve as a 'portal' to particles in the so-called 'Dark Sector'. The FIP interactions might occur within the interactions of a 400 GeV proton beam with a beam dump used in this experiment.
The neutrino background consists of particles emerging from neutrino inelastic interactions with the detector material, especially with the decay vessel walls and the gas inside of the decay vessel. Only those interactions that can mimic a FIP interaction are considered as background signal. It is elaborated on the criteria on which the relevant interactions from the given data set are selected. Furthermore it is explained why the background from inelastic neutrino interactions is insignificant for the measurements, with conservatively estimated less than 0.001 significant events in the whole time of operation of the SHADOWS experiment.

Zusammenfassung

Diese Arbeit behandelt die Analyse des Untergrunds aus inelastischen Neutrino Wechselwirkungen für ein neues "Proton Beam Dump" Experiment namens SHADOWS (Search for Hidden And Dark Objects With the SPS) mithilfe von Monte Carlo Simulationen. Ziel des Experiments ist sogenannte Feebly Interacting Particles (FIPs) zu finden. Diese könnten potentiell den experimentellen Beweis für mehrere wichtige Theorien liefern und als "Portale" zu Teilchen im sogenannten "Dunklen Sektor" dienen. Die FIP- Interaktionen treten möglicherweise bei den Interaktionen eines 400 GeV Protonenstrahls mit einem Beam Dump auf, welcher in diesem Experiment verwendet wird.
Der Neutrino-Untergrund besteht aus Teilchen, welche hervorgehen aus den inelastischen Neutrino Wechselwirkungen mit dem Detektormaterial, insbesondere mit den Wänden und dem enthaltenen Gas des Zerfallsvolumens. Nur Wechselwirkungen welche ununterscheidbar zu FIP Wechselwirkungen sind, werden als Untergrund Signal gewertet. Es wird darauf eingegangen nach welchen Kriterien die relevanten Wechselwirkungen aus dem Datensatz selektiert wurden. Ebenfalls wird beschrieben warum der Hintergrund aus inelatischen Neutrino Wechselwirkungen konservativer Abschätzung nach, mit weniger als 0.001 zu erwartenden ereignissen in der gesamten Laufzeit des SHADOWS Experiments, nicht signifikant für die Messungen ist.

Contents

Chapter 1

Introduction

The search for new particles started with the discovery of the electron[1] as well the mechanisms of nuclear fission and nuclear fusion in 1939[2][3]. Since then, thousands of physicists pursued the goal to understand the fundamental structure of matter and it is still an ongoing field of research. One of the biggest milestones has been the formulation of the standard model theory (SM), the leading model of particle physics in the early 1970s. Great efforts have been made to extend this model and to answer open questions in physics which can not be explained with the SM. The SHADOWS experiment takes part in those efforts with the goal to find new Feebly Interacting Particles (FIPs) which can provide a 'portal' to particles in the so-called 'Dark' or 'Hidden Sector'. These are yet unobserved hypothetical particles which do not interact via the known interaction modes of the SM (electromagnetic, strong and weak interactions). SHADOWS is a fixed target proton beam dump experiment, which is currently in the proposal phase. It is planned to be connected to the Super Proton Synchrotron (SPS) at the European Organisation for Nuclear Research (CERN).
In the aftermath of the beam hitting the dump FIPs can emerge. By detecting the visible decay products of these FIPs their existence could potentially be verified.
This thesis covers the analysis of the background signal, induced by inelastic neutrino interactions with the SHADOWS detector material using a Monte-Carlo (MC) simulation. This analysis was done in the context of the Technical Proposal for SHADOWS [4].
To provide a basis for the later parts of this thesis in Chapter 2 the basic concepts of the SM and FIPs are described. In Chapter 3 the different detector components of the SHADOWS detector are explained. There will also be a short description of the beam line. Some basic properties and methods regarding the MC simulation are explained in

Chapter 4. In Chapter 5 the neutrino background study is discussed, which is the centerpiece of this thesis. The background signal is then compared to expected signals in Chapter 6, which is interesting regarding the significance of the simulated background.

Chapter 2

Standard Model and Feebly Interacting Particles

Standard Model

The SM is well tested and explains most of the occuring phenomena in particle physics. It is wrapped around three fundamental forces namely the weak, electromagnetic and strong force[1] [5] and sorts all known particles in different categories which are depicted in Figure 2.1.

With half integer spin both leptons and quarks are per definition fermions. Those elementary fermions have been categorised into three generations where each includes two differently charged quark-flavours, as well as a lepton with its corresponding neutrino. The particles in the higher generations are (in general) characterised by a shorter lifetime and greater mass. Thus, they are likely to decay into the lower generation particles.
The bosons serve as force carriers for interactions of elementary fermions. Bosons are divided into vector bosons and the higgs boson, the only scalar boson. The vector bosons are defined by their integer spin, whereas the higgs boson has a spin of zero. Every elementary particle also has a corresponding anti particle which is not listed in Figure 2.1. The anti particles have the same properties as their corresponding particles, with the exception of them having opposite charges. Here, not only the electrical charge is meant but also others as the color charge of quarks for example. Every quark possesses one of 3 charge like quantum numbers, which mediates the strong force.

[1] The gravitational force is not regarded in the model.

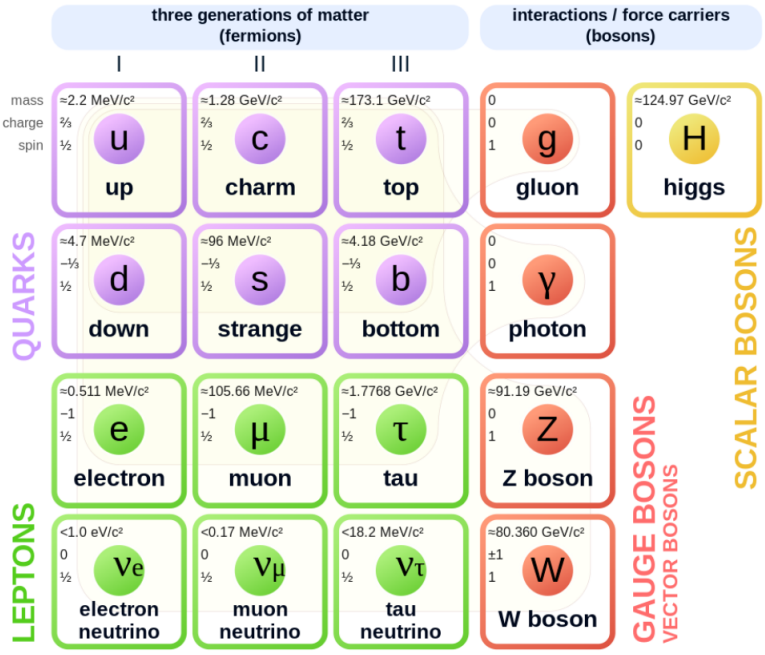

Figure 2.1: Standard Model of elementary particles containing six quarks and six leptons as well as four vector and one scalar bosons. Quarks and leptons can be divided into three generations. Each particle is shown with its mass, charge and spin. [6]

Although the SM is successful in reproducing experimental results, it is not considered to be perfect or complete [7][5]. Huge efforts are made to answer open questions in particle physics that cannot be explained with the SM (⇒physics beyond the standard model). These questions address for example the existence of dark matter, the neutrino mass or why there are exactly three generations of fermions. To answer these open questions further research is needed. The search for FIPs is part of these efforts.
To find those new elementary particles which are not included in the SM, collisions and interactions with high energies are needed. These are made possible with the particle accelerators at CERN near Geneva.

Feebly Interacting Particles

FIPs are supposedly mediating particles which could provide a connection between SM particles and particles in the so-called 'dark' or 'hidden' sector which posses neither weak, electric or color charges. Besides from interactions via FIPs these dark sector particles would interact via gravitational force. Hypothetical examples for FIPs could be axions, other Axion-Like-Particles (ALPs), dark photons, dark higgs or Heavy Neutral

Leptons (HNLs). With 'dark', in general, a form of matter is refered to which seemingly do not interact with light or electromagnetic fields. Those interactions between SM and dark sector are categorised into several so-called 'portals'. The most important interaction portals are shown in Table 2.1. This chapter is based on informations from [8] and [9].

Detection Methods

There are different approaches for the detection of FIPs (and DM in general) which cover a broad range of possible FIP masses (up to TeV) and experimental methods.

- FIPs coupled to SM particles can potentially have *visible decays*. This means that the products from these interactions can be detected. It mostly occurs with ALPs or HNLs. Because of the low interaction rate of these FIP decays high intensities are needed, and with that also a high background signal can be expected. For this kind of FIP decays mostly proton beam dump experiments are used (a list with different experiments and their FIP sensitivities is shown in Figure **??** of the Appendix, but this detection method is applied in nearly all FIP-searching experiments.

- For invisible decays of long-lived FIPs the *missing momenta and energies* of visible particles involved in the decay can be used to obtain information about the FIPs. For this the momentum and energy of the visible particles has to be known before and measured after the FIP interaction. This detection method is mostly used at fixed target experiments.

- Another detection method measures the *missing mass* in a known decay. For example a e^+e^- interaction where a photon and a dark photon emerge. In this case mass would be missing, if only the the visible particles are considered. Since the initial momentum of the particles has to be known this method is mostly used in collider experiments. For this method to work the detector needs a very good hermeticity so none of the emerging (visible) particles stay undetected.

- Furthermore, *electron scattering from light DM* in the detector material can be measured directly. For this, electron or proton beam dump setups are used. A

downside of this method is the large electron/proton intensity needed because of the small electron scattering probability and the similarity to the signal of neutrino interactions.

Portal Formalism

The different interactions between the SM and the dark sector particles can be categorised with so-called interaction 'portals'. Every portal is corresponds to a Lagrangian $L_{portal} = \Sigma O_{SM} \times O_{DS}$, which combines operators from the SM fields with their interaction partners of the dark sector fields. All of the possible operator combinations for one sort of interaction are summed up to make up one 'portal Lagrangian'. The Lagrangians of four of these portals are listed in Table 2.1. More information about the different portals can be found in [9],[10] and [8] .
Each of the four portals listed in Table 1 is the basis of a physical model which can solve some of the open questions in particle physics.

Portal	Decay modes
Scalar portal	$\ell^+\ell^-$, $\pi^+\pi^-$, K^+K^-
Pseudo-scalar portal	$\ell^+\ell^-$,$\gamma\gamma$, $\pi^+\pi^-$, K^+K^-
Vector portal	$\ell^+\ell^-$, $\pi^+\pi^-$, K^+K^-
Fermion (neutrino) portal	$\ell^\pm\pi^\mp$, $\ell^\pm K^\mp$, $\ell^\pm\rho^\mp(\rho^\mp \to \pi^\pm\pi^0)$, $\ell^+\ell^-\nu$

Table 2.1: Main FIP decay modes into visible final states through the four shown portals where $\ell = e, \mu, \tau$ and ρ is the rho meson. Table adapted from [8].

- The *vector portal* or 'dark photon portal' includes interactions of FIPs that have spin 1 with new fermions or new scalars. These FIPs would be the 'dark equivalents' of the gauge bosons depicted in Figure 2.1. The coupling happens through kinetic mixing [11] which is a phenomenon in which for example a dark photon, which is the most predicted FIP for this portal, can 'change' into a regular photon.

- The *scalar portal* or also-called higgs portal includes interactions of scalar FIPs, that have even parity, with the dark sector. Since the only scalar particle in the SM is the higgs boson (Figure 2.1) interactions within this portal happen via kinetic

mixing of the higgs with the dark higgs.

- The *Fermion (neutrino) portal* includes interactions including Heavy Neutral Leptons. It is theorised that there is one HNL for each of the different neutrino generations [12]. Between the neutrinos and their corresponding HNLs can possibly occur mixing phenomena. In cosmology and astrophysics the HNLs have been suggested to be promising DM candidates and could provide an answer for the existence of neutrino masses.

- The *Pseudo-scalar portal* concentrates on interactions with the SM through pseudo-scalar fields. Pseudo-scalar particles with odd parity and a spin of zero could interact with dark sector particles trough this portal. These pseudo-scalars could be axions and axion-like particles. The existence of axions would solve the strong CP-problem. In theory the CP (Charge-Parity) symmetry does not hold for strong interactions but no such violation of symmetry could yet be observed. [13]

FIP detection at SHADOWS

SHADOWS is designed to reconstruct a range of different FIPs, for this it concentrates on the detection of visible final states from FIP decays. SHADOWS has not only sensitivity for one of the interaction portals specifically. As shown in Table 2.1, visible decays are possible through all portals. Possible FIPs that could be detected indirectly by detecting those decay products would for example be axions and axion-like particles, dark higgs or HNLs. Some exemplary decays are shown in Figure 2.2.
The SHADOWS setup is based on a proton-beam dump with a 400 GeV proton beam. The FIPs potentially produced at these energies would most likely result from charm and beauty hadron decays. Those hadrons have just a small boost at the center-of-mass energy of the SPS ($\sqrt{s}$ = 28 GeV), which also means that the FIPs will have a large polar angle when they emerge. That is also one of the reasons why the SHADOWS detector is placed off-axis in respect to the beam line.

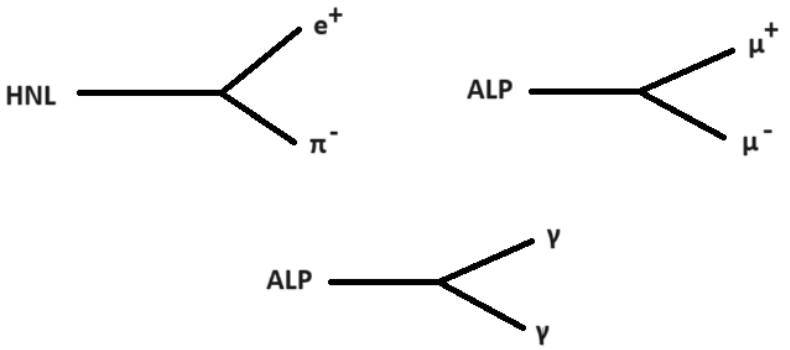

Figure 2.2: Exemplary decays of HNLs and ALPs into visible final states which could potentially be detected with the SHADOWS detector.

Chapter 3

SHADOWS Detector

The following chapter is based on the SHADOWS Technical Proposal [4] for the SPSC (Super Proton Synchrotron Comitee), where the SHADOWS detector is described in detail.

3.1 Location

The SHADOWS detector is planned to be located uptream of the T10 target at the CERN North Area complex in the TCC8 tunnel that leads to the ECN3 experimental hall. During operation, the proton beam from the Super Proton Synchrotron (SPS) is delivered to the T2, T4 and T6 targets and protons that did not interact at T4 and T6 are transported to the T10 target in front of SHADOWS. The SHADOWS experiment is proposed alongside the HIKE (High Intensity Kaon Experiments) experiment [15]. This is the proposed successor of the NA62 experiment currently located in the complex. NA62 as well as HIKE are kaon experiments.

3.2 Beam line

Since HIKE is a kaon experiment, two beam modes are needed to allow both SHADOWS and HIKE to be operated using the same beam line. In kaon mode, the T10 beryllium target will produce a K^+ beam as it currently does for NA62. In beamdump mode, the T10 target will be lifted up and the 400 GeV proton beam will be delivered on a Target Attenuator for Experimental areas (TAX) dump collimator, which is copper-iron based. It originates from NA62 and will have to be adapted for higher intensities. The TAX has

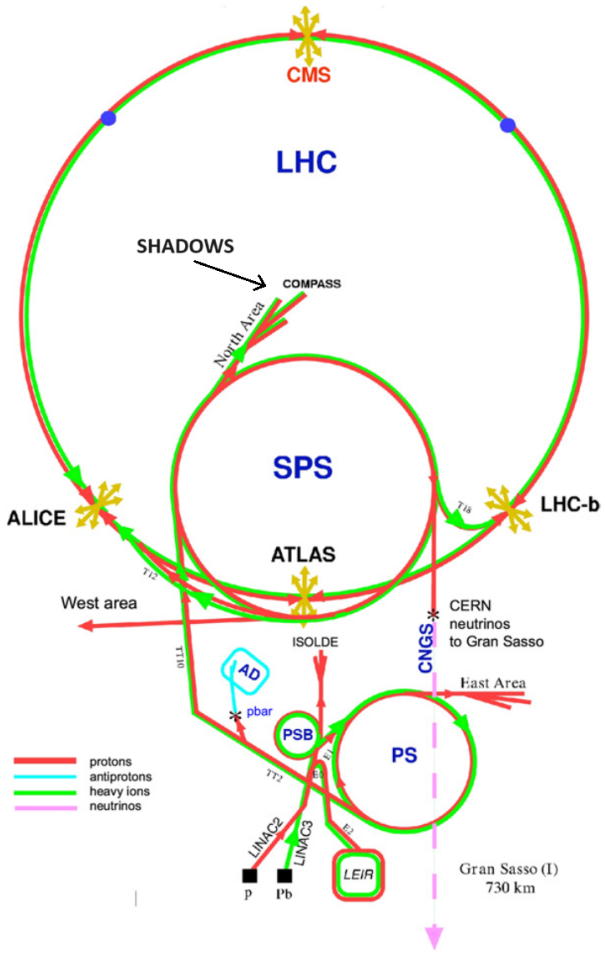

Figure 3.1: Overview of CERN complex with the Large Hadron Collider (LHC) as well as the Super Proton Synchrotron (SPS). The creation of the proton beam for SHADOWS starts at the LINAC2 linear accelerator then the protons are lead trough a booster (PSB) and are fed into the Proton Synchrotron (PS) where they are accelerated up to 25 GeV. At last they are injected into the SPS and after further acceleration passed to the north area complex. Graphic adapted from Ref.[14].

a small hole for the kaons to pass through during kaon mode. In beam-dump mode however, the TAX is moved in a way where all of the particles are dumped. In Figure A.1 of the appendix the beam line with the TAX is shown in more detail.

The detector is planned to be placed off-axis from the beam line to the left of the beam direction (shown in Figure 3.1). This is because the FIPs will have a large polar angle when they emerge, additionally the background is reduced[1]. Furthermore without this off-axis configuration the SHADOWS detector could not coexist with HIKE.

[1]In general the particles which could induce background signals emerge with a smaller polar angle.

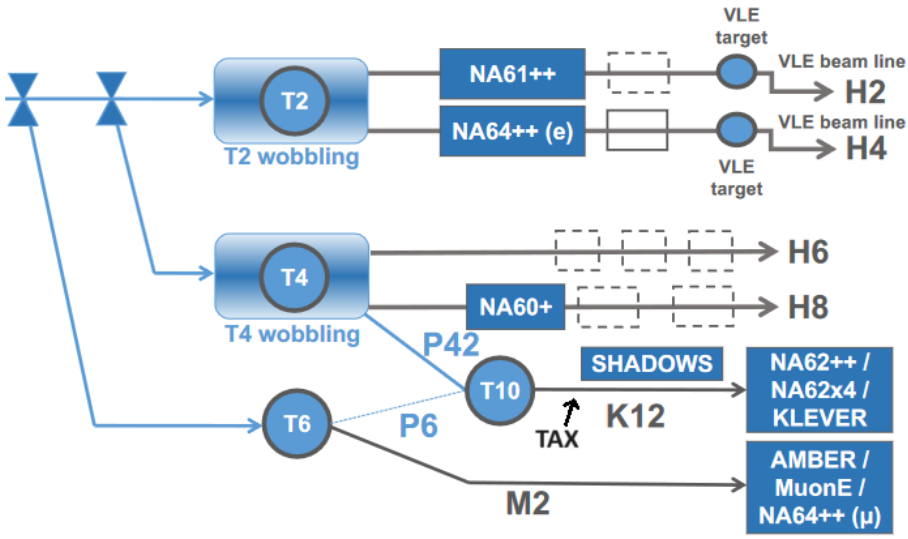

Figure 3.2: Overview of CERN north area beam lines. The proton beam from the SPS is delivered to targets T2,T4 and T6. Protons which did not interact on T4 and T6 are passed to the T10 target. In beam dump mode this target is lifted and the beam is dumped on the Target Attenuator for Experimental areas (TAX) in front of SHADOWS. Figure taken from Ref.[16]

.

3.3 Geometry and detector elements

A mix of particles emerges from the dump, some of them in the direction of the detector. In front of the detector a muon sweeping system is planned which is composed of Magnetised Iron Blocks (MIBs) to heavily reduce the muon background in the experiment. The muons are diverted out of the detector acceptance. After most of the muons have been swept away, the rest of the particles are lead to the decay vessel. If there are decays with visible final states inside of the the decay vessel, those can be registered and the decays reconstructed.

MIB system

To sweep away the muons, especially those in the acceptance of the SHADOWS tracking systems, and to avoid a substantial muon background, MIBs have been installed in the first part of the SHADOWS setup. In Figure 3.4, the system of MIBs arranged around the decay vessel is shown. The first two dipole magnets (depicted in yellow) have been implemented not for SHADOWS but for HIKE. They reduce the muon background for HIKE in beam dump mode. The stage 1 magnet has the purpose to split the incom-

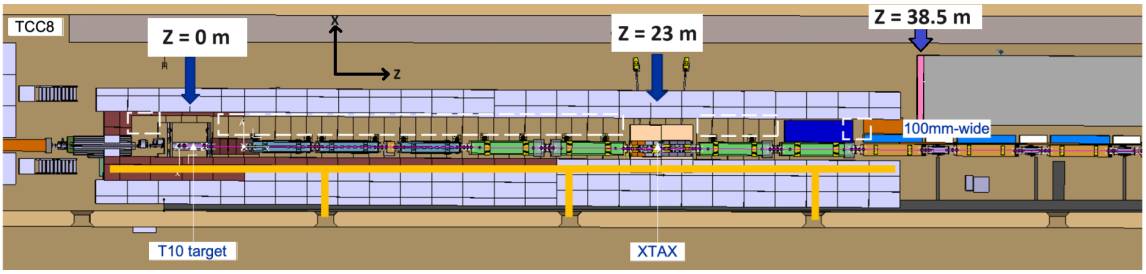

Figure 3.3: Beam line components in top view. The roof shielding is removed to show them. The blue components to the right from the T10 target are quadrupoles and the green components are dipole magnets. At z = 38.5 m the beginning of the decay vessel is depicted. Figure adapted from Ref.[4].

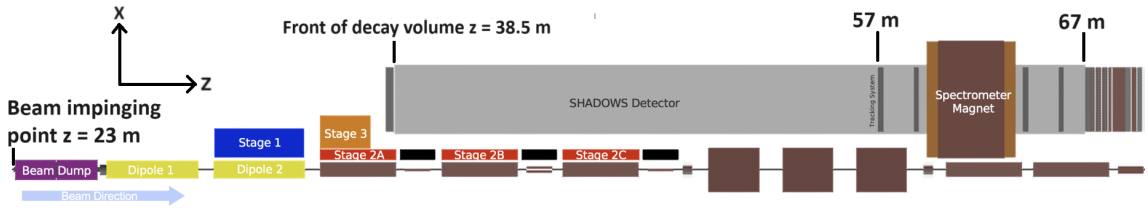

Figure 3.4: Detector Geometry with muon sweeping system using MIBs. The stage 1 magnet divides the muons by charge along the y-axis and the stage 2 and 3 magnets sweep them away along the x-axis. All measurements are given in respect to the origin at the T10 target. The side wall of the detector facing the beam line starts at x = 1.37 m. Figure adapted from Ref.[4].

ing muons by their charge, along the y-axis. The stage 2 and stage 3 magnets are then supposed to sweep the divided muons out of the detector acceptance and off to the side along the x-axis. The three stage 2 magnets are alternated with non magnetised iron-blocks which just provide passive shielding. In Figure 3.5, it is shown how the MIB system effects the muon background. In this way, the muon flux can be reduced by a factor of around 70 from 147 MHz to 2 MHz [4].

Decay vessel and veto system

The decay vessel is approximately 19 m long and has a 2.5 m × 2.5 m cross section. It is planned to hold a vacuum of about 1mBar. A helium balloon is also an option that is actively discussed. It would be cheaper and furthermore it would increase the acceptance, because it would be closer to the beamline. Also inelastic interactions inside of the vessel walls could be prevented since the balloon would be made from very thin PVC.

Some of the muons from the dump are not sorted out by the MIB system. At the front

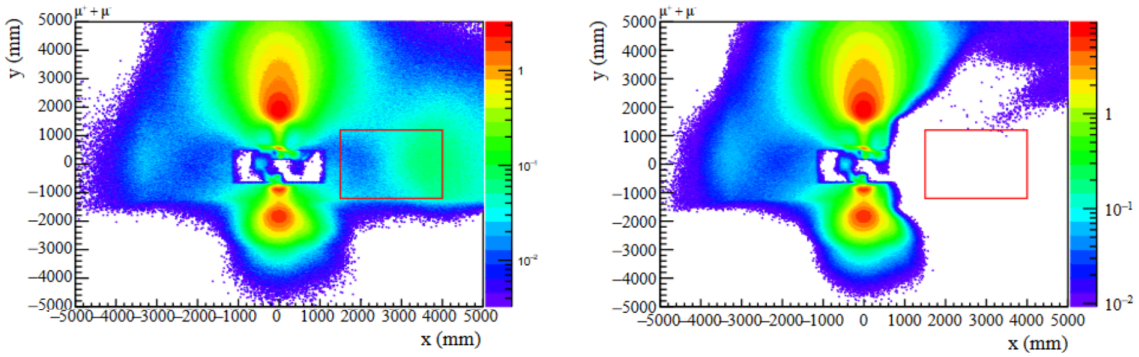

Figure 3.5: Effect of MIB system on muon flux at the z-plane of the first tracking station. The upper structure results from μ^+ particles while the lower structure is based on μ^- particles. The red box depicts the position of the tracking station. In this area both μ^+ and μ^- particles occur. Flux reduction from 147 MHZ to 2 MHZ can be achieved. Figure taken from Ref. [4].

and on one side of the decay vessel, a veto system will be installed to detect those muons and other charged particles resulting from interactions with the MIBs. It is planned to consist out of two layers of Micromegas. With those implemented, charged particles which enter the decay vessel might still be detected by the tracking system. However they can be sorted out afterwards because they already have been detected by the Micromegas in the veto system. The two layers of Micromegas have an expected efficiency greater than 99.8%, a spatial resolution in the order of millimeters, a time resolution in the order of 10ns and a rate capability of up to 10 $\frac{\text{MHz}}{\text{cm}^2}$ [4].
The measured events are supposed to take place inside of the decay volume. The decision to add a veto system on the side of the vessel is based on the results of the background simulations. It was noticed that there was a considerable amount of interactions in the side wall of the vessel. The veto system on the side wall is not planned to be implemented along all of the 19m of the vessel, though it will probably only cover the first 2.5 m^2 of the wall. However, the optimal measurements have yet to be studied.

Tracking System

The four tracking stations that the system consists of are supposed to retrace the path of charged particles inside of the decay vessel. By analysing these tracks, the underlying decays can be reconstructed. This includes precise reconstruction of the position of the decay vertices and the mass of the decayed particle, respectively a FIP.
The tracking stations each have two stereo-layers (for x and y axis separately). Each of these two layers is proposed to be made out of two straw tube layers.

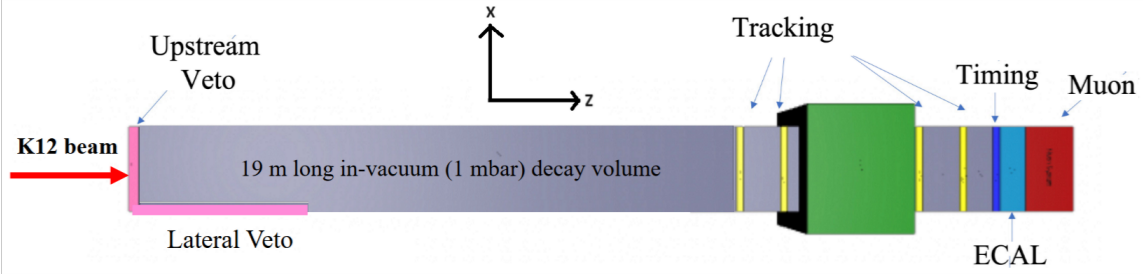

Figure 3.6: SHADOWS detector geometry in top view without the MIB system. The dipole magnet is depicted in green. ECAL stands for Electromagnetic Calorimeter. The decay volume has a cross section of 2.5 m × 2.5 m. Figure adapted from Ref.[4].

An alternative with scintillating fibres is being considered. However, since the option with the straw tubes has a better cost effectiveness this is the currently chosen main option. The tracking system is expected to have a resolution of around 1% for mass measurements a vertex resolution of 0.5 to 4.5 mm in x-direction and 0.2 to 1 mm in y-direction and a impact parameter resolution of around 3 mm [4].

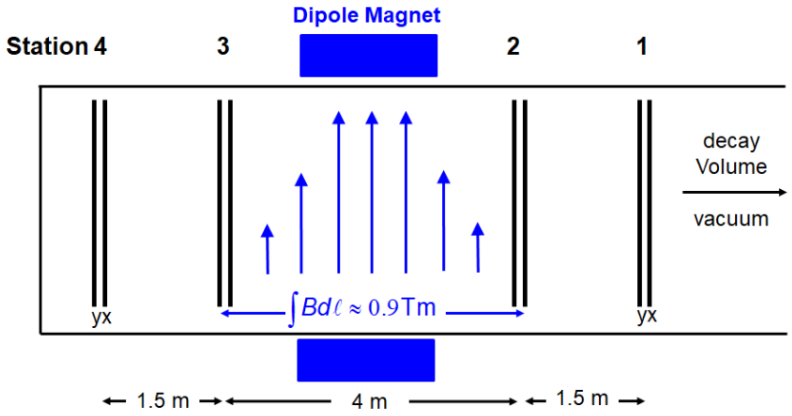

Figure 3.7: The four tracking stations with the dipole magnet inbetween. The dipole magnet has an integrated field strength of 0.9 Tm. Each of the stations consists of stereo layers for the x and y direction separately. Figure taken from [4].

Dipole Magnet

Charged particles are bend away from their original paths inside of the magnetic field of the dipole magnet. By tracking this change in direction, information regarding the charge and mass of the particles can be gained. Two options for this magnet have been discussed. One 'warm' option is proposed with warm meaning that the magnet func-

tions in ambient temperature conditions and one superconducting option. An integrated field strength of around 1 Tm in y-direction is required. The dipole magnet is possibly the biggest cost factor in the setup which motivates the decision to propose the warm option since it is cheaper.

Timing Detector

The most important task of the timing detector is the tracking of background muons in cooperation with the muon detectors. If two muons hit the timing detector and the muon system with a time difference higher than the time resolution of 100ps they do not count as a signal, because they do not result from the same decay. Most of the background is removed with this resolution. By further improving it the cost efficiency would worsen.
The detector is proposed to be made out of scintillating bars. For the readout, Silicon Photo Multipliers (SiPMs) will be implemented by mounting them on both sides of a plastic scintillator bar (8 SiPMs per bar). The measurements will then be taken with Application-Specific Integrated Circuits (ASICs) on readout boards. The whole timing detector will include 200 of these bars with the dimensions $126\times6\times1\text{cm}^3$ [4].

Electromagnetic Calorimter

The ECAL is supposed to detect also neutral decay products like photons which emerge from FIP decays like ALP $\rightarrow \gamma\gamma$. Furthermore it identifies electrons, pions and photons like the muon system does for muons. From precise energy measurements, the FIP mass can be determined. For the reconstruction of the decay vertices from neutral decay products, the shower direction has to be identified. For this the calorimeter is split into multiple layers (pointing capability).
The electron identification efficiency is demanded to be greater than 99%, the energy resolution has to be in the range of 10 to 15%, and the pion misidentification rate is required to be lower than 1% [4]. Different alternatives which fulfill these requirements have been considered.
Based on the results of the simulations it has been concluded that an option with thin scintillating strips (StripCal) fits best in terms of cost efficiency and pointing resolution. With the StripCal option, the ECAL would then consist out of 40 iron layers alternating with readout layers with 250 scintillator strips each. The readout can be realised with

one SiPM and a wavelength-shifting fibre (WLS) at each end of a strip.

Muon Detector

The detection and identification of muons is important for rejecting background muons. This can be done in combination with timing measurements as explained above. The detection is supposed to have a efficiency higher than 95% [4]. The system is proposed to be made out of scintillating tiles which will be organised in modules (16 or 32 tiles per module). Eight of those modules will be mounted onto one station. Each tile is read out by four SiPMs. There will be three stations in total. These tiles have a time resolution of about 250 ps.

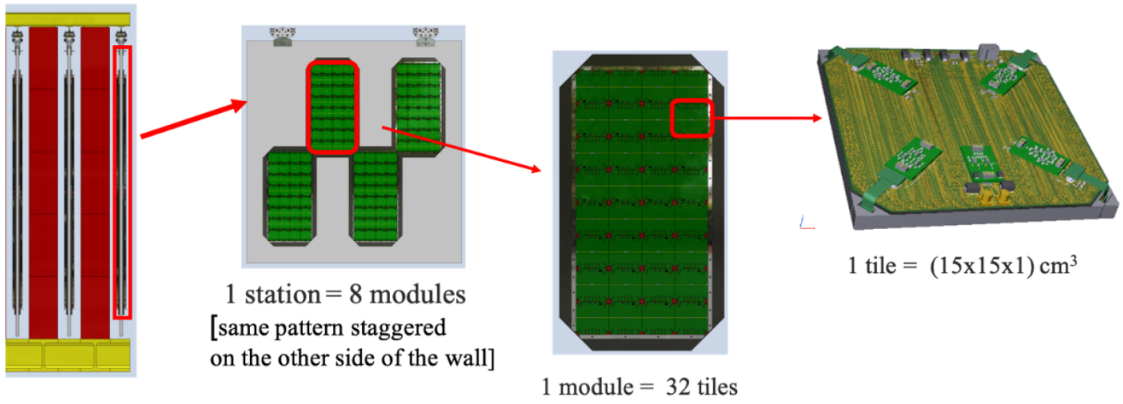

Figure 3.8: Muon system composed out of 3 stations with each having eight modules comprised out of 16 or 32 tiles each. Figure taken from [4].

Chapter 4

Monte Carlo Simulation

The SHADOWS MC simulation is based on the GEANT4 NA62 MC framework [17]. It simulates the interactions between particles and the detector components. The signal is produced with PYTHIA8 [18] and the background with the GEANT4 based BDSIM package [19]. The signal and the background data is then passed to the MC framework. The following chapter is based on the SHADOWS Technical Proposal [4], where the MC framework and the different simulation methods are described in more detail.

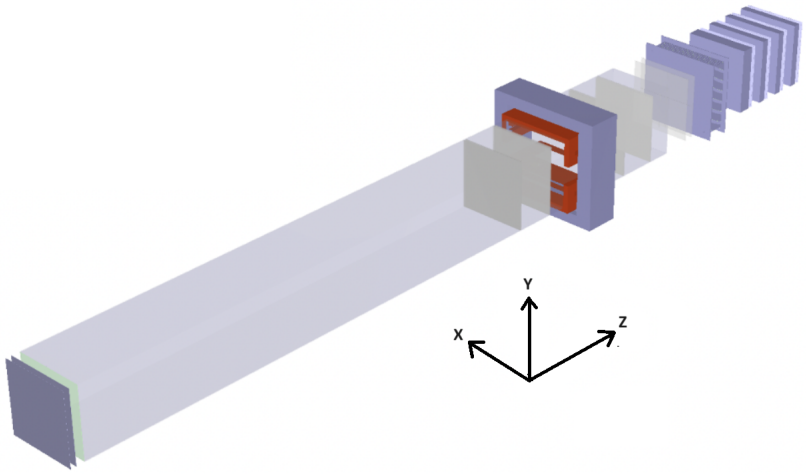

Figure 4.1: SHADOWS geometry used in the MC. The lateral veto has not been included. Figure taken from [4].

Beamline and detector elements

The simulation of the K12 beamline is GEANT4 based (BDSIM) and includes the TAX dump and all of the magnetic elements and collimators needed to control the beam.

The simulation also considers interactions between protons and the beamline materials.
All of the detector elements described in the previous chapter have been implemented in the simulation with exception of the lateral veto which has been proposed based on the results of the background simulations.

Detector	In MC implemented options
Upstream veto	Micromegas
Tracking chambers	straws
Dipole Magnet	warm option
Timing detector	Scintillating bars
ECAL	StripCal
Muon System	Scintillating tiles

Table 4.1: Detector elements implemented in MC. The lateral veto is not included. Table adapted from [8].

Reconstruction

The reconstruction process involves measurements with the tracking system and the ECAL, depending on the decay[1]. The reconstruction with the tracking system uses the methods explained below.

- The *tracks* are reconstructed by performing a linear fit for the x-z and the y-z plane. For the x-z plane however, the track has to be fitted in front of and behind the dipole magnet separately. From the angle between the reconstructed tracks the momentum of the particle can be calculated.

- The *vertices* can be reconstructed by extrapolating the tracks back to their intersection point. Since in the y direction there is no deviation in the path of the tracks, the reconstruction resolution is better than in the x direction. For vertices which are further away from the trackers, the resolution is worse.

- The *Impact Parameter (IP)* is reconstructed by summing up the momenta of the tracked particles and trace them back from their common vertex to the point

[1] For instance a FIP decaying into two pions would be reconstructed based on measurements from the tracking system and for a decay into two photons it would be reconstructed with the ECAL data.

which is closest to the beam impinging point on the dump. The IP is the smallest distance between this point and the particle path which has been traced back shown in Figure 4.2.

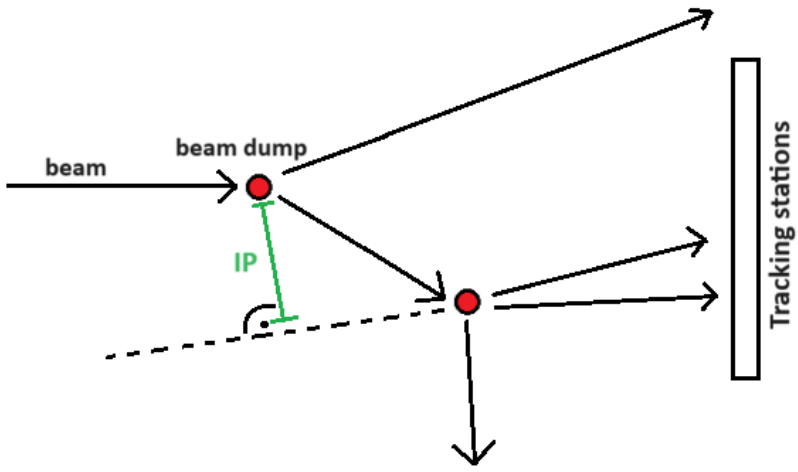

Figure 4.2: Determination of the impact parameter. The momenta of the detected final states from one event are summed up and traced back. The closest point between this track and the beam dump is defined as the Impact parameter. FIPs are in general produced still inside of the beam dump and their IP is therefore in most cases below 6cm (see [4] or Chapter 6).

From a simulation with ALPs (600 MeV) decaying into two muons the total reconstruction efficiency has been determined to be 83% [4]. For this total efficiency, the vertex and tracker reconstruction efficiencies, as well as the impact parameter efficiency and the acceptance rate have been considered.

The reconstruction with the ECAL uses a different approach. From a hit, showers are formed inside the ECAL. The shower products hit multiple scintillating tiles in different layers. These hits on the tiles are then grouped into different clusters. The direction of the clusters and with that also the direction of the shower can then be fitted.

Signal Studies

The expected signal are FIPs resulting from the decay of hadrons containing beauty or charm quarks. These decay, still being in the dump because of their short decay lengths. For analysing the different FIP signals, the MC framework is able to create a range of

FIPs[2]. The reconstruction efficiency for FIPs was estimated based on ALPs decaying into two muons. The total reconstruction efficiency for ALPs has been determined to be 82.8% [4]. Similar values are expected also for other FIPs.

[2]These are created outside of GEANT4 and are then passed over to prevent problems with the GEANT4 physics list.

Chapter 5

Inelastic neutrino background

The analysis of the muon and neutrino background are essential for validating the expected signal. Only with a estimation of the background, it can be assured that the possibly observed events are actually FIP decays. The expression 'neutrino background' comprises the final state particles that result out of neutrino inelastic interactions with the detector and beamline components. The combinatorial background, where particles from different interactions hit the tracking system at the same time within the timing resolution is neglectable within the given data set. This will get clear at a later point of the analysis.
These inelastic interactions result from neutrinos interacting with the different detector and beam line components. Most of these neutrinos emerge from kaon and pion decays and it is mostly muon neutrinos (58%) and anti muon neutrinos (38%) [4]. From these neutrinos approximately 7% enter the decay volume which is to be expected due to the off-axis placement of the SHADOWS detector.

Neutrino Sample

The inelastic neutrino interactions were generated using the GENIE event generator [20]. It simulated approximately $3 \cdot 10^8$ Protons on Target (POT) but the sample is statistically equivalent to $5 \cdot 10^{19}$ POT because in the simulated sample, interactions between the neutrinos and the detector components (especially with the decay vessel) are forced to occur. A POT of $5 \cdot 10^{19}$ POT is expected in the whole SHADOWS lifetime.
This amount of POT results in $3.6 \cdot 10^5$ neutrino interactions which includes both elastic and inelastic interactions. For each of the neutrino interactions the sample includes the parameters shown in Table 5.1. One neutrino event has multiple assigned entries with

data from singular particles which take part this interaction. This data stems from simulation and not all of these parameters, like the weight or the multiplicity of an event could always be reconstructed in an actual praxis run.Two exemplary inelastic neutrino events are shown in Table 5.3 and 5.4.

Parameter	Description
Production Points	Location of the decay vertex that the respective particle emerged from. Multiple decays can happen in one inelastic neutrino event.
PDG-ID (Particle Data Group Identification)	Identification number from which the type of particle can be determined.
Momentum	Given in x-, y- and z-direction. This is how the direction of the particle tracks can be determined.
Weight	Represents the probability of a neutrino interaction taking place without forcing. All particles in one neutrino interaction get assigned the same weight. Elastic neutrino interactions get assigned a weight of 1.
Multiplicity	Number of particles that are involved in one neutrino interaction.

Table 5.1: Parameters included in neutrino sample. Each neutrino interaction in the sample has assigned entries containing data from the particles that take part in the interaction.

Selections

To determine the background signal, the inelastic neutrino interactions contained in the neutrino sample have to be evaluated in relation to their significance. Significant are only those events which produce a signal that could be mistaken for a FIP decay. Events which are not relevant have to be disregarded, this is done by defining different selection criteria. Different combinations of these criteria are applied together in so-called 'selections' to evaluate their respective effects. After applying all of the criteria at once, the events that are left compose the expected background signal. The selection criteria that will be applied in this analysis are listed below. There could be derived even more criteria, but these are sufficient for ruling out all of the simulated neutrino events in terms of potential background signals.

- *Weight:* By demanding the weight that is attached to each neutrino interaction in the sample to be smaller than 1, elastic interactions do not get selected. This requirement is applied for all of the performed selections.

- *Geometric selection:* The selected events are required to include production points which are located inside of the decay vessel. This can include or exclude the decay vessel side walls, the reasoning behind the distinction will be motivated later on. This criterion is used in all of the performed selections.

- *Event multiplicity:* The selected neutrino events are demanded to have a multiplicity of two or higher to be able to produce a signal similar to a FIP signal. Particles with production points outside of the geometric requirements and particles which do not fulfill the momentum requirement are not regarded in the determination of the multiplicity. Thereby the primary neutrinos are not considered. This requirement is demanded in all of the performed selections.

- *Momentum:* Particles are required to have a momentum above 3 GeV, otherwise they do not get accounted for when determining the multiplicity of an event. This momentum marks the energy threshold of the tracking systems, it is the minimum momentum required for muons to hit the third muon station. This requirement is only applied in the second selection in Section 5.2. In all of the other selections performed, particles are just required to have a positive momentum. This is supposed to exclude particles with a momentum of zero.

- *Hits on tracking stations:* The particles in the selected events, are demanded to hit all four tracking stations of the tracking system. This would be necessary for a reconstruction of the decay. Particles which do not fulfill this requirement are not considered when determining the event multiplicity. This would also be required for particles that are reconstructed with the ECAL and muons which have to hit the muon stations, since they still have to pass through the tracking system. The ECAL can detect if particles come in from the side and the muon stations need to work together with the timing detector. This requirement does not exclude intermediate particles or particles with to small momenta to hit the relevant detector elements. The tracks of the respective particles are just extrapolated onto

the tracker planes. The magnetic field of the dipole magnet was accounted for. This requirement is demanded only in Section 5.3.

- *Impact parameter:* To be similar to a FIP decay the IPs of the decays included in a neutrino interaction that are selected is required to be smaller than 6 cm [1]. A FIP can also be partially reconstructed if secondary events resulting from FIP decays are reconstructed. In consideration of such a case an IP smaller than 40 cm can also be demanded as selection criterion [4]. This criterion is applied in a subsection of Section 5.1.

Additional selection criteria that could potentially be applied, if these listed above would not succeed in separating out all of the events would be:

- Neglection of *intermediate particles*, which are not remaining after the neutrino interactions. These are particles which decay into other particles before reaching the trackers. However, the primary particles produced outside of the decay vessel (muon neutrinos and muons) at 38.05 m are excluded from the selection process through the geometric requirements, so this would only apply for secondary events. Examples for such particles are shown in table 5.2. A π^0 for example could never be detected in this setup, having a lifetime in the magnitude of 10^{-17}s.

- Since the main decay modes of FIPs include decays into two *oppositely charged particles* or two photons, this kind of decay products could also be demanded from the selected events. An overview of the different decay modes is given in Table 2.1.

5.1 Geometric Selection

The first selection reduces the total amount of events down to those which include production points inside of the decay vessel or in the decay vessel walls. Furthermore, the neutrino events are demanded to have a multiplicity of two or higher, wherefore particles with a momentum of zero and particles with a production point outside of the decay vessel are not considered.
For this selection it is not important if the particles emerging from those interactions

[1] According to simulations around 96-98% of the generated FIPs with fully reconstructed decay vertices, had an IP of lower than 6 cm [4]. Different FIP masses were considered for this simulation.

could actually be tracked or the underlying events reconstructed.
After applying these selection criteria, 203 inelastic neutrino events remain. All of the following studies included in Section 5.1 are performed for these selected events with these specific selection requirements.

Production Points

In Figure 5.1 the production points included in the 203 neutrino events discussed above can be seen. This amounts to 299 production points, due to secondary events. In the x-z-diagram the lateral wall of the decay vessel can be recognised which is on the side facing the beamline. In the y-z-diagram, it can be seen that the points are more evenly distributed. This is because the front and not the top of the decay vessel side wall is shown. Most of the interactions take place inside of the wall. The decay vessel starts at z = 38.5 m and the first tracking station is located at 57 m[2], whereby the origin is located at the T10 target at (0,-0.023,23.07) m. All of the production points have to be located in this z-range of the vessel. In the y-x-diagram the points are shown out from the perspective of the first tracking station looking in the direction of the upstream veto at the front. The shown production points are accumulated over all y (top left), x (top right) and z (bottom) values inside of the decay vessel. To understand these histograms better it is helpful to compare them with Figure 3.4 or Figure 3.6 where the geometry of the detector is shown.

Hits on trackers

In Figure 5.2, the hits of the particles from the selected events, on tracking station 1 (left) and station 4 (right) can be seen. The tracking requirement would demand that the particles hit all four stations, however for this it is sufficient to just observe the hits onto station 1 and 4. It can be seen that on tracker 4, there are substantially less particle hits, this alone can indicate that only few of those events would fulfill the requirement if it would be applied.
To depict the hits, the given direction of the momentum of the emerging particles was just extended linearly onto the respective tracker station plane. For the hits on station 4 the effect of the dipole magnet on charged particles was considered.

[2]Exact detector measurements can be seen in Figure A.2 of the appendix.

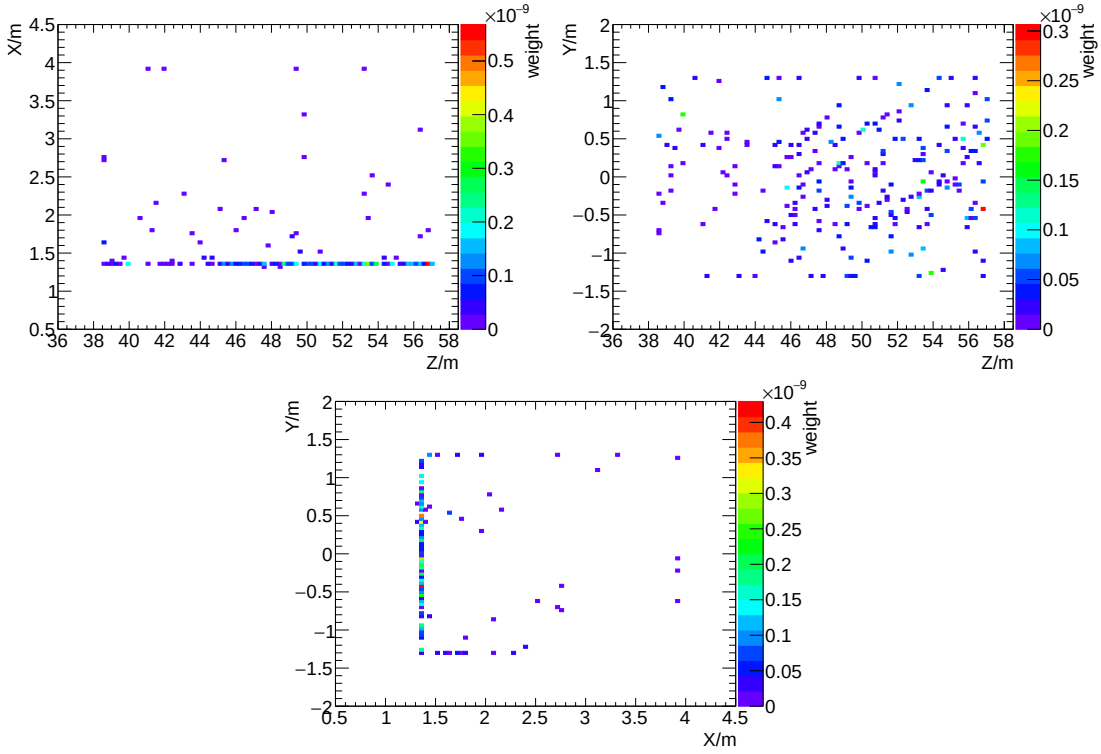

Figure 5.1: Positions of decay vertices inside of the decay vessel or the decay vessel walls. The structures that can be recognised originate from the interactions within the vessel walls, mostly the wall facing the beamline at $x = 1.37$ m.

Probability distribution

In Figure 5.3 the probability distribution of all selected neutrino interactions can be seen. For each event, one weight is filled into the diagram. Most of them are in the region of 10^{-11} to 10^{-12}.

By summing up the probabilities the number of expected inelastic neutrino events during the lifetime of the detector can be assessed. This results in $1.189 \cdot 10^{-9}$ events per $3 \cdot 10^8$ POT, which amounts to $\frac{1.189 \cdot 10^{-9} \cdot 5 \cdot 10^{19}}{3 \cdot 10^8} \approx$ **198 inelastic interactions** in $5 \cdot 10^{19}$ POT. This is equivalent to $8.25 \cdot 10^{-5}$ events per spill with $2.4 \cdot 10^6$ spills in total.

Particle distribution

By summing up all the particles of the same type their relative occurrences can be compared. In Table 5.2 the distribution of the 1124 particles from the selected events is

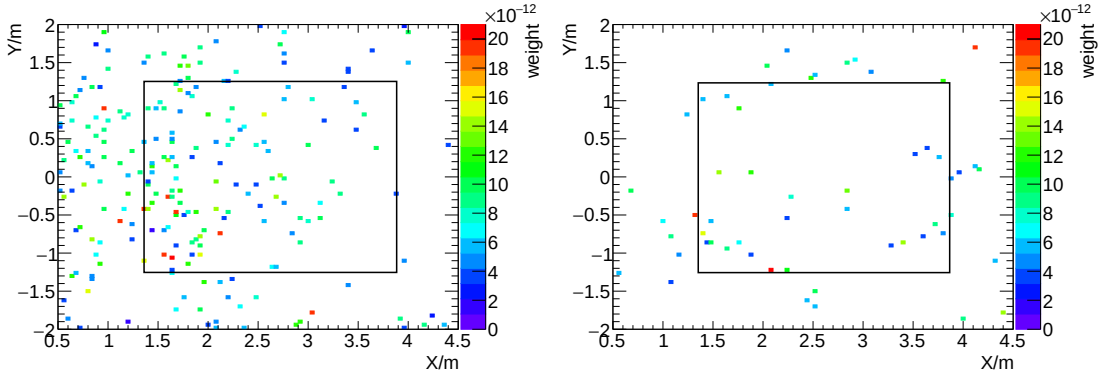

Figure 5.2: Hits on tracking stations 1 (left) and 4 (right). For this, the points of intersection between the particle tracks and the z-plane of the tracking stations were calculated. Station 1 is located at approximately 57 m and station 4 at 64 m (for exact values see Figure A.2 of the appendix). The black box marks the tracker acceptance.

shown. These are not all of the particles included in the neutrino interactions, it is just those for which the event got selected for regarding the location of the production points. The primary neutrinos and muons are not included for example. However these particles could also include intermediate ones like the π^0 as mentioned before. The majority of these particles are neutrons, which could potentially pose background signals in the ECAL. Interesting particles included in the table in regard of mimicking a FIP decay, would be for instance oppositely charged pions, muons and electrons some exemplary decays are shown in Figure 2.2.

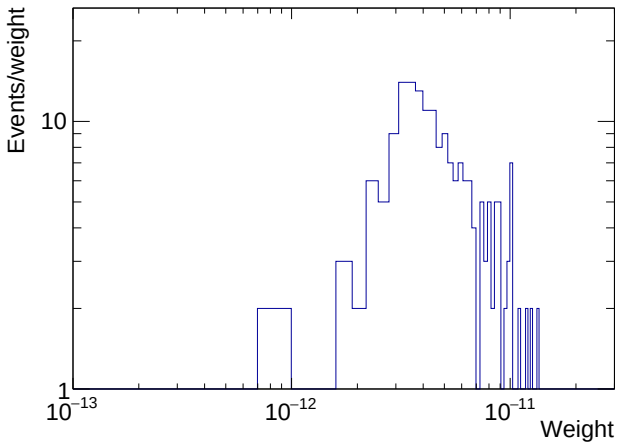

Figure 5.3: Probability distribution for geometric selection. Summing up the weights results in $1.189 \cdot 10^{-9}$ events per $3 \cdot 10^8$ POT.

Particle	Number of particles	expected Lifetime in s (only magnitude)
n	363	$\sim 10^{2}$
μ^-	199	$\sim 10^{-6}$
π^0	138	$\sim 10^{-17}$
p	113	
π^+	91	$\sim 10^{-8}$
γ	88	
π^-	47	$\sim 10^{-8}$
ν_μ	43	
μ^+	10	$\sim 10^{-6}$
K^0	7	
Λ	6	$\sim 10^{-10}$
K_S^0	5	$\sim 10^{-10}$
K_L^0	5	$\sim 10^{-8}$
K^+	4	$\sim 10^{-8}$
$\overline{K^0}$	3	
Σ^+	2	$\sim 10^{-10}$
D^0	1	$\sim 10^{-13}$
e^+	1	
In total 1124 particles from 203 events		

Table 5.2: Particle distribution of the 1124 particles that the 203 neutrino events got selected for. Neutrons make up for the biggest part but there are also many muons and pions which can be interesting regarding the similarity to a FIP decay. Also some intermediate particles are included in the selection. More information on the lifetimes can be found in [21].

Impact Parameter

The IPs are calculated by summing up all the momenta from the particles, included in the selected events which have a common production point inside of the decay vessel. The direction of this momentum is then traced back to the point which is closest to the beam impinging point (shown in Figure 4.2).

In Figure 5.4 the smallest IPs are below the 40 cm that are required for a FIP decay to be partially reconstructable. Additionally applying the requirement for the IPs to be smaller than 40 cm would leave 6 of of the 203 neutrino events left. Summing up their weight results in $3.90 \cdot 10^{-11}$ expected events in $3 \cdot 10^{8}$ POT, which amounts to $\frac{3.90 \cdot 10^{-11} \cdot 5 \cdot 10^{19}}{3 \cdot 10^{8}} \approx$ **6.5 inelastic interactions** in $5 \cdot 10^{19}$ POT. This number is important for the later assessment of the total expected background signal.

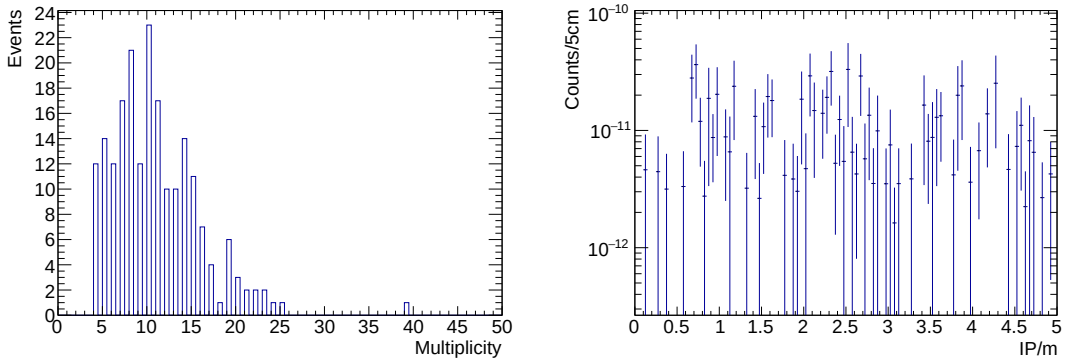

Figure 5.4: Multiplicity and IPs of the selected events. The multiplicities are that high because the selected events are often made up out of secondary events. In the right figure the IPs of all the selected events are shown.

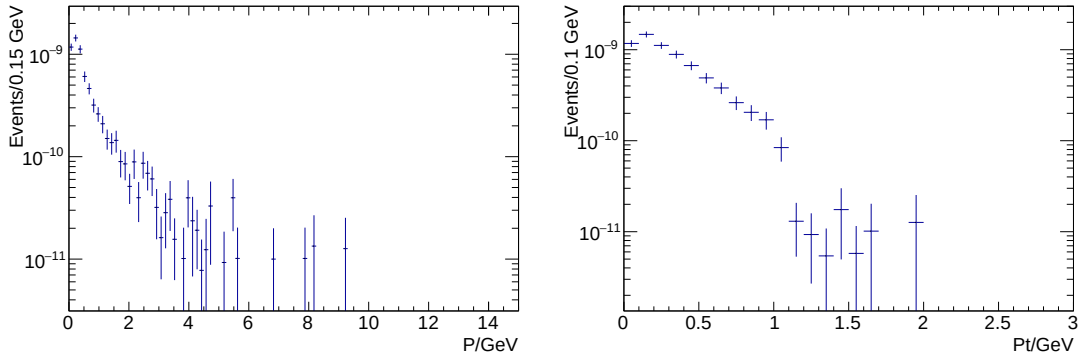

Figure 5.5: Initial Momentum (left) and initial transverse momentum (right) of final states from the selected events. The transverse momentum is the momentum in the x-y plane whereas the momentum P is defined in 3d space ($\vec{P} = \vec{P}_t + \vec{P}_z$).

5.2 Geometric and Momentum Selection

For the second selection the same spacial and multiplicity requirement as in Section 5.1 is applied, which means that at least two particles have to emerge out of the production points included in one neutrino interaction. This has to take place inside of the decay vessel or the decay vessel side walls. In addition to that the momentum requirement is now applied. The emerging particles will now need a total momentum higher than 3 GeV to be considered regarding the multiplicity of an neutrino event. Only two events

are left after applying these criteria. The production points of these events can be seen in Figure 5.6, they are located in the side wall of the decay vessel[3]. At this point further selections would not be sensible anymore and the two events can just be evaluated further by looking at their respective particle compositions to tell if those events could potentially produce a background signal.

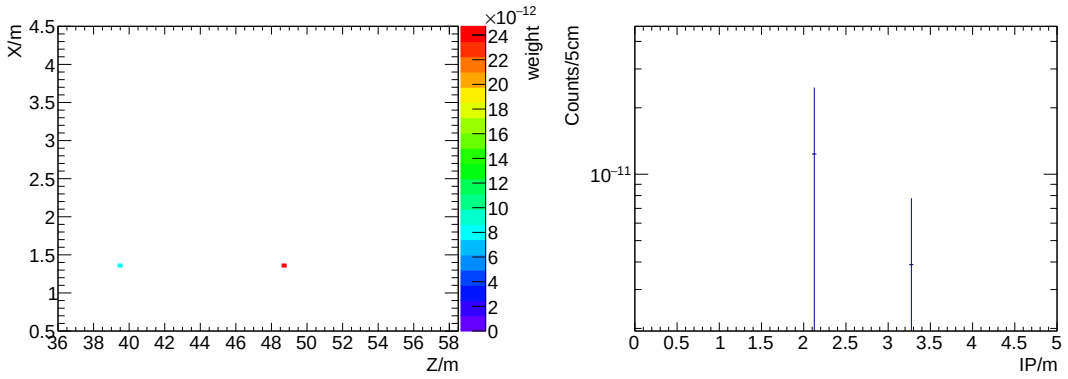

Figure 5.6: On the left the two Production points are shown that are left after applying the additional 3 GeV momentum cut. On the right, the IP can be seen, both values are located way above the required 40cm to be similar to a partially reconstructable FIP decay.

The full particle composition of the two selected events is shown in Table 5.3 and Table 5.4. In each of the selected events two particles have a momentum greater than 3 GeV and were produced inside of the vessel. Of course none of these events would actually be reconstructable, considering their short lifetimes. The π^+ particle in Table 5.4 presumably decays into the anti-muon and the muon neutrino labeled with event ID five but those do not have enough momentum left to overcome the 3 GeV requirement. The π^0-particle seemingly decays into photons. The two Kaons are also unable to produce a fake FIP signal. This means that no events are left for applying further selection criteria.

Combinatorial Background

At this point in the analysis it becomes clear why the combinatorial background can be neglected. From the 1124 Particles that were included in the 203 selected events in Section 5.1 only 42 even have a momentum greater than 3 GeV. From these 42 only 7 particles are actually hitting all of the tracking stations. Six of those are equally charged

[3] In x-direction the decay vessel starts at 1.37m

muons and one is a π^0 which is an intermediate particle. This could not be detected as a fake FIP signal. Even if there were oppositely charged muons, they still had to fulfill the requirement that the distance of closest approach of their tracks is below the vertex resolution of the tracking system. And they had to be tracked at the same time, within the time resolution of the timing detector.

Interaction composition					
Event ID	Particle	p [GeV]	prodx [m]	prody [m]	prodz [m]
1	ν_μ	6.43	1.24	0.35	38.05
2	$\overline{K^0}$	0.73	1.37	0.39	39.57
	K_L^0	0	1.37	0.39	39.57
	K^0	3.92	1.37	0.39	39.57
	K_S^0	3.92	1.37	0.39	39.57
	p	0.49	1.37	0.39	39.57
	μ^-	1.02	1.37	0.39	39.57
3	μ^+	7.08	-0.14	1.41	38.05
Weight: $3.89 \cdot 10^{-12}$					

Table 5.3: Particle distribution of the first of the selected events. The particles that this event got selected for are marked in blue. The other particles do not have more than 3 GeV or have a production point outside of the vessel.

Expected background signal

The two events that were left could be ruled out in terms of possibly mimicking a FIP decay, by examining their particle composition. However, at the latest they would have been sorted out after applying the IP requirement or demanding hits on all 4 tracking stations.

The probability of detecting background signals from inelastic neutrino interactions, which could mimick FIP decays, is consequently extraordinarily low. Because of the lack in statistics it cannot be determined how low exactly, but an assessment of the background signal can be made, based on the individual effectivity of the different selection criteria.

For this, the 'selection efficiency' of the momentum requirement applied in this sec-

tion, is compared to the efficiencies of two other selection criteria with low relative dependencies[4]. All of these selections use the same geometric requirements used in Section 5.1). Then in addition to that the requirement for hits on all tracking stations will be applied, but no longer the 3 GeV cut. This selection is performed in the following section. The other selection will apply the geometric selection and additionally demand the IPs to be smaller than 40cm. This selection already has been performed in Section 5.1. Combining the effectivities of these three requirements will yield an estimation of the magnitude of the expected background events, since these requirements are mostly independent.

If just the result of the selection performed in this section is considered, neglecting the previous evaluation of the particle composition, an expected background could be assessed nevertheless. The two selected events result in $1.63 \cdot 10^{-11}$ events per $3 \cdot 10^{8}$ POT, which would amount to $\frac{1.63 \cdot 10^{-11} \cdot 5 \cdot 10^{19}}{3 \cdot 10^{8}} \approx$ **2.71 inelastic interactions** that could be expected in the lifetime of the detector. This is equivalent to $1.13 \cdot 10^{-6}$ events per spill. Therefore the momentum requirement reduced the amount of background signals from 198 to 2.71 by a factor of **73**.

[4] A rough estimation of the dependencies between the different criteria is performed in the appendix.

Interaction composition					
Event ID	Particle	P [GeV]	prodx [m]	prody [m]	prodz [m]
1	ν_μ	13.40	0.79	0.08	38.05
2	μ^+	0	1.358	0.156	48.662
	ν_μ	0.03	1.358	0.156	48.662
3	n	0.39	1.361	0.161	48.665
	n	0.07	1.361	0.161	48.665
	π^0	0.18	1.361	0.161	48.665
	γ	0.00	1.361	0.161	48.665
	γ	0.04	1.361	0.161	48.665
	π^+	0.41	1.361	0.161	48.665
	n	0.00	1.361	0.161	48.665
	π^+	0.00	1.361	0.161	48.665
	π^+	3.24	1.361	0.161	48.665
	π^0	4.60	1.361	0.161	48.665
	γ	0.00	1.361	0.161	48.665
	γ	0.00	1.361	0.161	48.665
	μ^-	0.18	1.361	0.161	48.665
4	μ^+	0.38	1.02	0.52	49.01
	ν_μ	0.04	1.02	0.52	49.01
5	μ^+	2.94	2.38	-1.23	54.54
	ν_μ	0.17	2.38	-1.23	54.54
6	μ^-	3.92	-0.25	1.18	38.05
Weight: $1.24 \cdot 10^{-11}$					

Table 5.4: Particle distribution of the second selected event. The two particles that this event got selected for are marked in blue. The other particles do not have more than 3 GeV or have production point outside of the vessel.

5.3 Assessment of total background in SHADOWS lifetime

To evaluate the magnitude of the expected background from inelastic neutrino interactions the same requirements as in the selection performed in Section 5.2 are applied. With the exception that the momentum requirement is revoked and replaced with the requirement of particles hitting all of the tracking stations. These two requirements do not have a high relative dependency, which is important for the validity of the assessment. An evaluation of these dependencies can be found in Chapter B of the appendix.

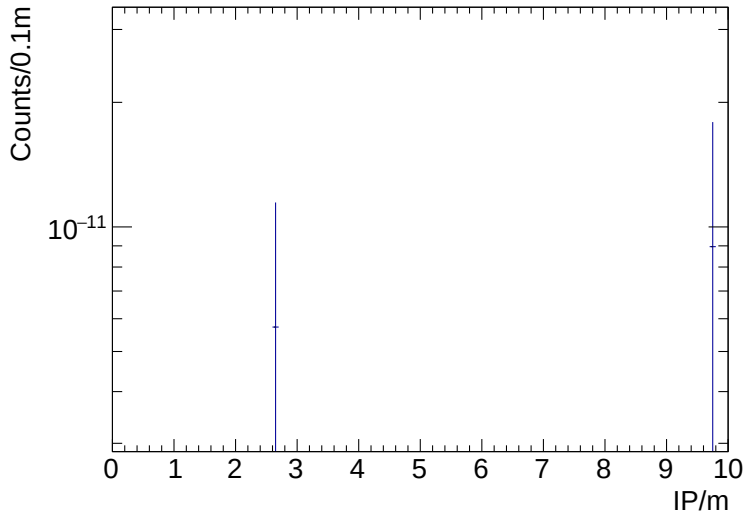

Figure 5.7: The impact parameters were calculated for the two trackable particles from each of the selected events. Those events contain more particles than those two but for the IP just these were considered since the simulation data is 'truce level data', so it includes informations that can not be gained in praxis runs. Only the particles which hit all four trackers would, if the momentum is above the energy threshold of 3 GeV, actually be detected. The IPs are not close to the 40cm required to be similar to a partially reconstructable FIP decay. In Figure 4.2 the determination of the IP is depicted.

After applying these criteria, again only two events are left. Their production points are not located in the area that the lateral veto would effect. They would not be reconstructable and could be sorted out by examining the particle compositions, or demanding a small impact parameter (shown in Figure 5.7). However, to determine the effectiveness of this criterion the assigned weights of the two events are summed up. This results in $1.47 \cdot 10^{-11}$ events per $3 \cdot 10^8$ POT which amounts to $1.47 \cdot 10^{-11} \cdot 5 \cdot 10^{19} / 3 \cdot 10^8 =$ **2.45 inelastic interactions** in $5 \cdot 10^{19}$ POT. This value is of comparable size as the num-

ber of expected interactions after applying the momentum selection (2.07 events).
This selection reduced the amount of selected events down from 198 to 2.45 expected events. This is a reduction with a factor of 81.

Combining the efficiencies of the momentum , the IP and the tracking criteria results in $198 \cdot \frac{2.71}{198} \cdot \frac{2.45}{198} \cdot \frac{6.5}{198} \approx \mathbf{0.001}$ events that could be expected during the lifetime of the detector. Of course this is just an assessment of the upper limit of events, the actual amount of events that can be expected is probably lower.

5.4 Evaluation of alternative option with helium balloon

To evaluate the quality of vacuum needed inside of the vessel, another selection is performed. The difference to the other selections is the exclusion of all events that take place inside of the vessel walls. The motivation behind this exclusion is the low amount of interactions that could be expected in the thin PVC walls of an helium balloon. The momentum requirement and the requirement for the particles to hit all of the tracking stations is not applied. After applying this criteria 8 neutrino events are left.
Since the decay vessel walls have been excluded from the selection no structure can be observed in Figure 5.8. From these selected events there are none which would actually be reconstructable as shown in the previous selections.

Summing up the probabilities of the events results in $4.18 \cdot 10^{-11}$ events per $3 \cdot 10^{8}$ POT this results in $\frac{4.18 \cdot 10^{-11} \cdot 5 \cdot 10^{19}}{3 \cdot 10^{8}} = \mathbf{6.97\ events}$ in $5 \cdot 10^{19}$ POT. This is equivalent to $2.9 \cdot 10^{-6}$ expected events per spill.
This neutrino background study was performed using air at atmospheric pressure inside the decay vessel. Since no events are left when applying the 3 GeV cut (shown in Figure 5.9), before even applying the other selection requirements, it can be assumed that the proposed vacuum of approximately 1mBar might not be needed and helium would be a viable option.

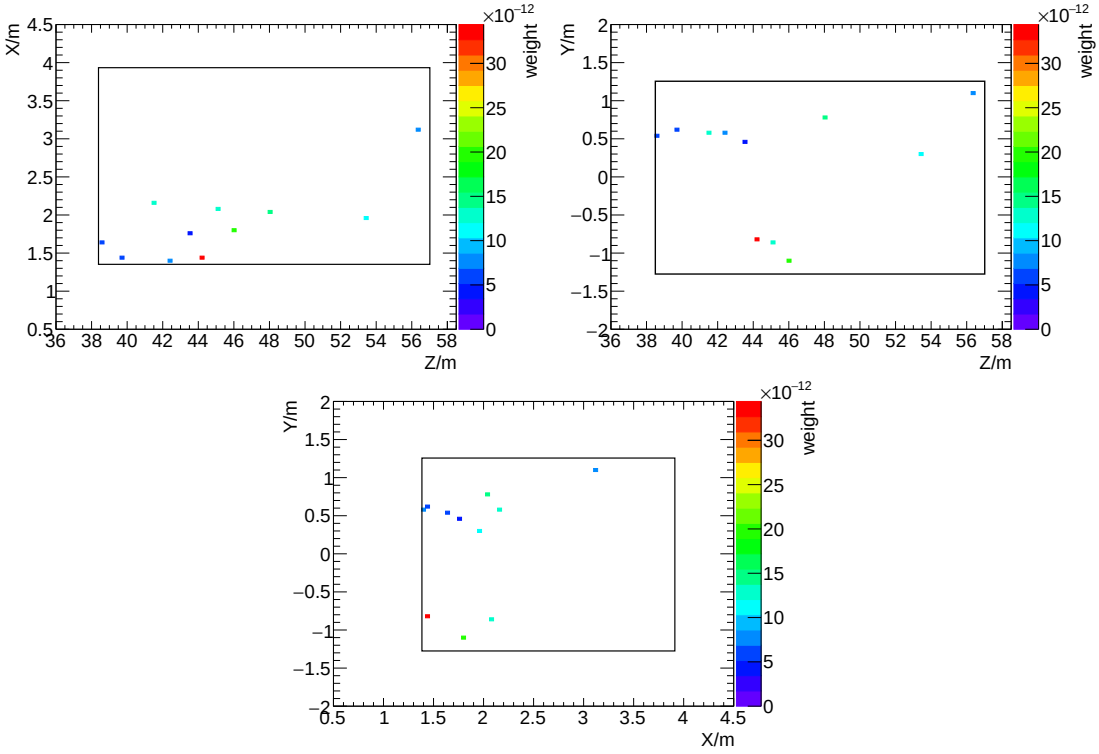

Figure 5.8: Positions of the decay vertices from the neutrino inelastic interactions inside of the decay vessel excluding the walls. 11 decay vertices from 8 neutrino events have been selected. The black frame suggests the position of the decay vessel walls.

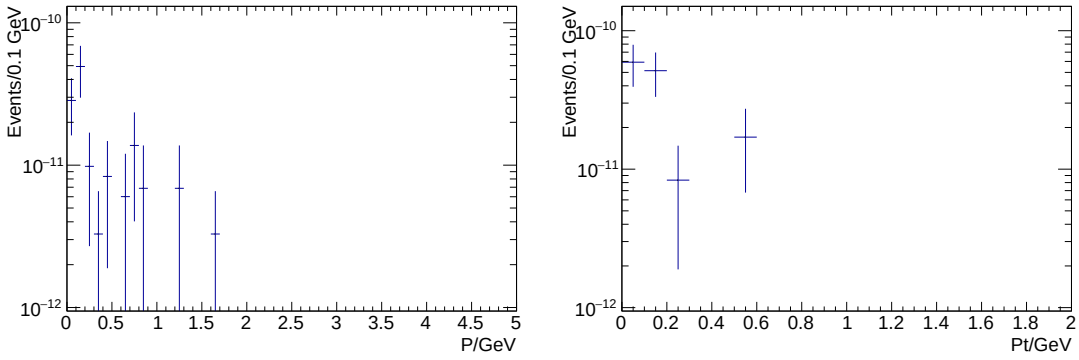

Figure 5.9: Initial Momentum (left) and initial transverse momentum (right) of particles from the selected events. The transverse momentum is the combined momentum in the x-y plane. None of the particles in the selected events have a momentum above the 3 GeV threshold.

Chapter 6

ALP signal study

To compare the results of the background study with data from actual signals, and to better understand the motivation behind the different selections that were applied, it seems natural to perform a study with actual signal data.
For this study three different ALP decays were analysed. ALPs decaying into two oppositely charged muons, two oppositely charged electrons and two photons. This does not exclude cases in which additional particles appear but in most of the decays in the sample it is just those which appear. In Table 6.1 the event compositions are shown.

Sample composition

The signal samples with e^+e^- and $\gamma\gamma$-production include 10.000 ALP decays each, however the sample with the $\mu^+\mu^-$-production includes 100.000 ALP decays. They are composed of mostly the same parameters as the neutrino background sample from the previous chapter. They include production points, particle IDs (PDG-IDs), and momenta of all particles that take part in the interactions. These interactions also include the primary b mesons from which the ALPs emerge (sketch of typical decay shown in Figure 6.1). In the simulation every ALP is generated in the vicinity of the beam dump and forced to decay into its respective final states in the z-range between 37m and 57m. For all three samples an ALP mass of 600MeV is used.

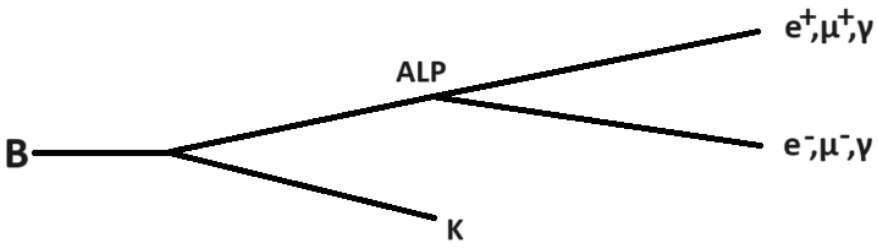

Figure 6.1: Feynman diagram of ALP decay. The alps are produced as part of the decay of bottom mesons. Such an exemplary decay into an ALP and a kaon is shown here. Later on, the ALP can potentially decay into the electrons muons or photons that are analysed in this case.

Distribution of final states in the ALP decays

Typical ALP decays that occur in the sample are depicted in Figure 6.1. But with such high momenta and energies, there are also occurrences where more than two final states emerge. For example an ALP decaying into more than 10 electrons, where the amount of electrons and positrons can be asymmetrical or an ALP decaying into two photons, as well as two electrons.

Momentum and IP selections

How the momentum and IP requirements which were applied in the last chapter effect the ALPs and the final state particles is shown in Table 6.2.
As for the impact parameter requirement of 6cm for full reconstruction and 40cm for partially reconstruction, roughly 92% of the ALPs have an IP lower than 6cm and nearly none at all have an IP above 40 cm. This result motivates the IP requirements that have been discussed in the previous chapter. These IP cuts exclude most of the background as could be observed and still most of the FIPs are not affected by it.
The momentum requirement was not implemented to reduce background, since it also reduces the signal events. For the sample which includes ALP decays into pairs of electrons, over half of the final state particles do not fulfill the 3 GeV requirement. The reason for this is that the energy does not get evenly split between the decay products and there are cases in which the ALP decays into more than two particles.

$ALP \rightarrow e^+e^-$		$ALP \rightarrow \gamma\gamma$		$ALP \rightarrow \mu^+\mu^-$	
Particle	Nr.of Particles	Particle	Nr.of Particles	Particle	Nr. of Particles
e^+	432	γ	392	μ^+	6936
e^-	430	e^+	5	μ^-	6931
		e^-	5	γ	97
				e^+	49
				ν_e	32
				$\overline{\nu_\mu}$	32
				n	20
				ν_μ	14
				e^-	9
				$\overline{\nu_e}$	7
				π^+	1
				π^0	1
				π^-	1
B^-	184	B^-	104	B^-	3298
B^0	105	B^0	45	B^0	1663
$\overline{B^0}$	87	$\overline{B^0}$	36	$\overline{B^0}$	1344
$\overline{B_S^0}$	28	$\overline{B_S^0}$	11	$\overline{B_S^0}$	625
ALP	404	ALP	196	ALP	6930
In total 1670		In total 794		In total 27990	

Table 6.1: Particle composition of all events where the ALP decays inside of the decay vessel coordinates. The muon sample is 10 times bigger but round about 18 to 35 times more ALP decays are observed than in the other samples.

Sample	IP		p		
	< 6 cm	< 40 cm	> 3 GeV		> 10 GeV
			ALPs	Final States	ALPs
$ALP \rightarrow e^+e^-$	92.17%	99.96%	97.64%	44.80%	87.50%
$ALP \rightarrow \mu^+\mu^-$	92.26%	99.99%	97.34%	84.92%	87.93%
$ALP \rightarrow \gamma\gamma$	92.15%	99.99%	97.07%	62.80%	87.52%

Table 6.2: Analysis of IP and momentum distribution in the three ALP samples. For this study the IPs off all ALPs in all three samples were determined. The amount of ALPs fulfilling the respective IP requirement is given in percent. For the evaluation of the momentum requirements also all of the ALPs and all of the final states included in the different samples were evaluated.

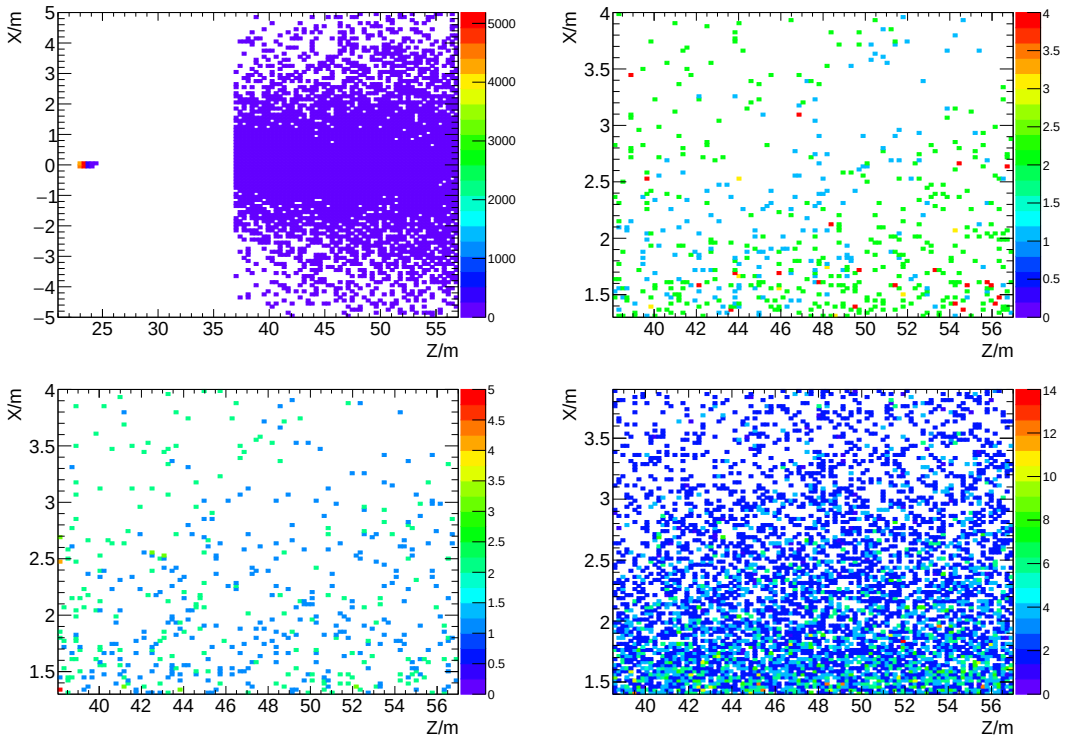

Figure 6.2: In the top left corner an overview is shown to clarify the points of generation of the ALPs around z = 23m (position of dump), as well as the production points which start at z = 37m[1], because those before 37m are irrelevant. The other histograms show the production points from ALP decays inside of the decay vessel for e^+e^- (top right),$\gamma\gamma$ (bottom left) and $\mu^+\mu^-$ (bottom right) decays. The counter on the right of each figure marks the number of events per point.

[1]The shown production points are plotted using the (ALP $\rightarrow e^+e^-$) sample. It looks very similar for the other decay channels.

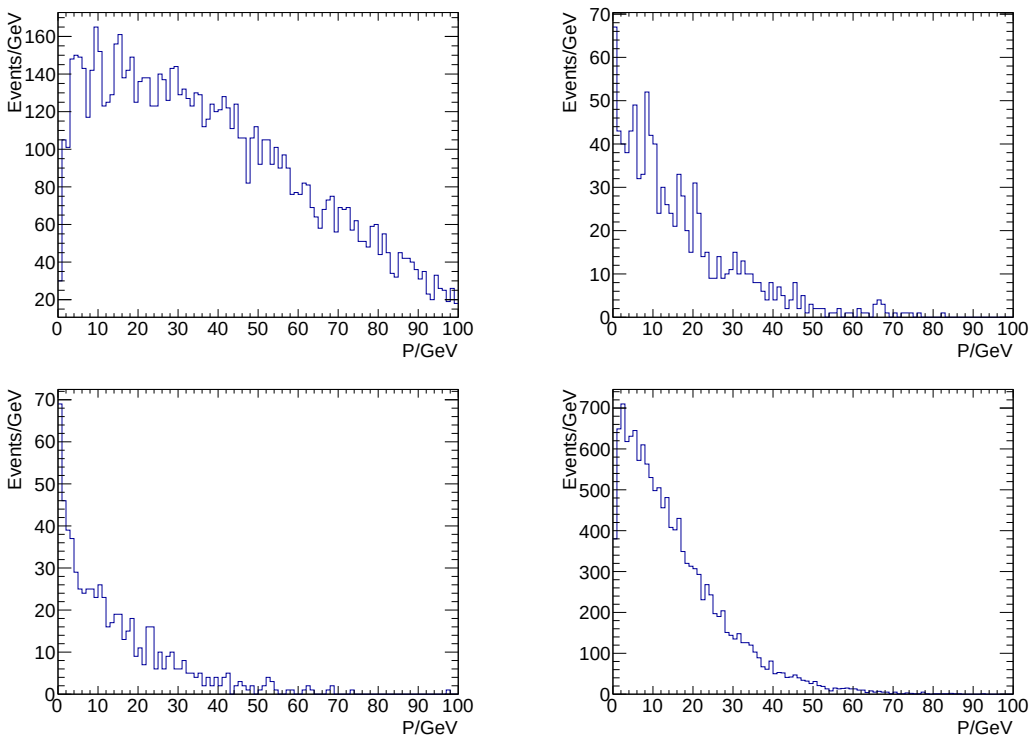

Figure 6.3: In the top left the momentum distribution of all the generated ALPs in the (ALP $\rightarrow$ e^+e^-) sample is shown, it looks similar in the other samples. In the other figures the distribution of momenta for the e^+e^- (top right),$\gamma\gamma$ (bottom left) and $\mu^+\mu^-$ (bottom right) decays are shown.

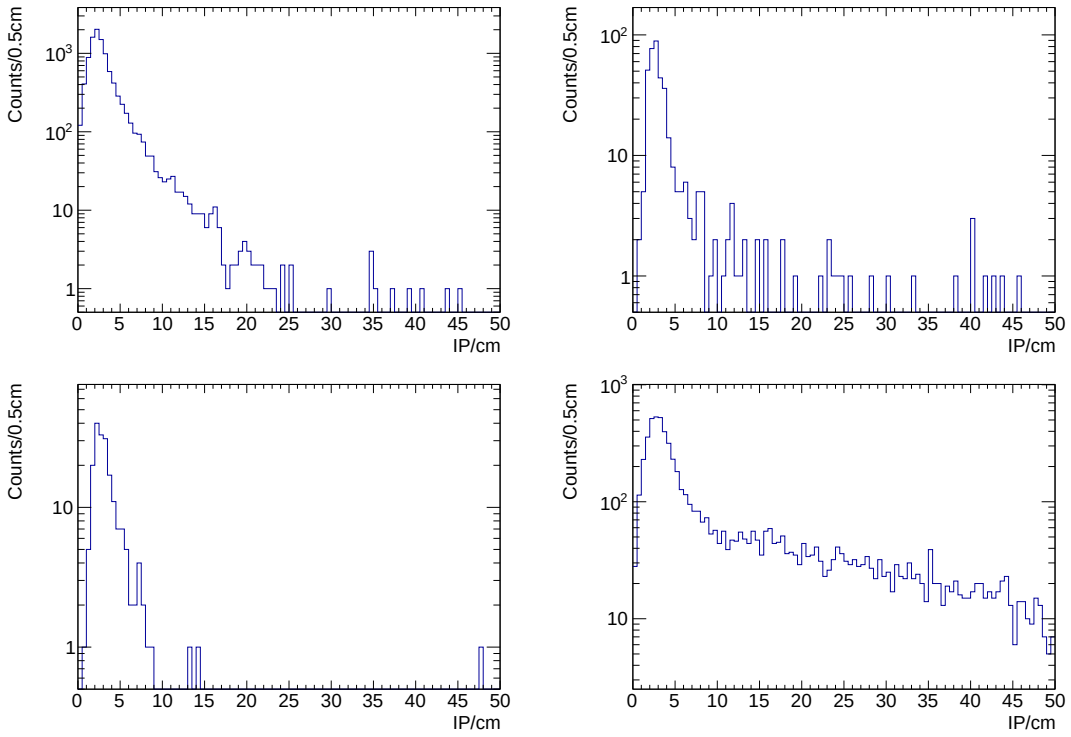

Figure 6.4: In the top left the impact parameters of all the generated ALPs in the (ALP $\rightarrow e^+e^-$) sample is shown, it looks similar in the other samples. In the other figures the impact parameters from the e^+e^- (top right),$\gamma\gamma$ (bottom left) and $\mu^+\mu^-$ (bottom right) decays, in the decay vessel including the walls, are shown.

Chapter 7

Conclusion and Results

The expected background signal from inelastic neutrino interactions for the SHADOWS proton beam dump experiment is not significant for the measurements. This can be shown by applying different criteria to select only significant events from the given neutrino sample. These significant events could potentially mimic the FIP decays that are supposed to be reconstructed by detecting their decay products.
Performing a geometric selection regarding the measurements of the SHADOWS decay vessel results in an expected number of inelastic neutrino events of **198** for the lifetime of the SHADOWS detector.
When in addition, a momentum requirement of 3 GeV for all particles is applied, which is the energy threshold of the SHADOWS detector, then **2.71** inelastic neutrino events can be expected to take place in the whole SHADOWS lifetime.
If the geometric selection is combined with the demand that all particles have to hit the four tracking stations of the SHADOWS tracking system, **2.45** inelastic neutrino events can be expected in the whole SHADOWS lifetime.
If the geometric selection is combined with the requirement that the IPs of the decays that take place have to be smaller than 40cm, **6.5** inelastic neutrino events could be expected in the SHADOWS lifetime.
Combining the 'event selection efficiency' of all three selection criteria, having a neglectable relative dependency results in less then **0.001** expected background events for the SHADOWS lifetime.
This background is not significant since 2.3 reconstructed FIP events would be necessary to achieve a certainty level of 90% that an actual FIP decay has been observed.
With another selection excluding events in the decay vessel walls it could be determined

that a helium balloon is a valid alternative to the decay vessel filled with a vacuum.

The analysis of three signal samples from ALP decays showed that 92% of the ALPs have an IP smaller than 6cm and almost all of them are smaller than 40 cm. Therefore the IP requirement applied in Chapter 5 seems valid.
It was determined that 97% of the ALPs possess a momentum higher than 3 GeV and 87% of them possessed a momentum higher than 10 GeV.
Many final state particles do not have the 3 GeV necessary to be reconstructable. In one sample it is less then 50% of the final states.

Appendix A

Additional reference material

Experiment	lab	beam	particle yield/$\mathcal{L}$	technique	portals	timescale
current						
ATLAS [119]	CERN	pp, 13-14 TeV	up to 3 ab^{-1}	visible, invis.	(1,2,3,4)	2042
Belle II [120]	KEK	e^+e^-, 11 GeV	up to 50 ab^{-1}	visible, invis.	(1,2,3,4)	2035
CMS [121]	CERN	pp, 13-14 TeV	up to 3 ab^{-1}	visible, invis.	(1,2,3,4)	2042
DarkQuest [122]	FNAL	p, 120 GeV	$10^{18} \rightarrow 10^{20}$	visible	(1,2,3,4)	2024
FASER [123]	CERN	pp, 14 TeV	150 fb^{-1}	visible	(1,2,3,4)	2025
LHCb [124]	LHC	pp, 13-14 TeV	up to 300 fb^{-1}	visible	(1,2,3,4)	2042
MicroBooNE [125]	FNAL	p, 120 GeV (NuMi)	$\sim 7 \times 10^{20}$ pot	visible	(2,4)	2015-2021
NA62 [46]	CERN	K^+, 75 GeV	a few 10^{13} K decays	visible, invis.	(1,2,3,4)	2025
NA62-dump [126]	CERN	p, 400 GeV	$\sim 10^{18}$ pot	visible	(1,2,3,4)	2025
NA64$_e$ [127]	CERN	e^-/e^+, 100 GeV	up to $1 \cdot 10^{13}$ e^-/e^+	$\not{E}$, visible	(1,3)	< 2032
PADME [128]	LNF	e^+, 550 MeV	$5 \cdot 10^{12}$ e^+ot	missing mass	(1)	< 2023
T2K-ND280 [129]	JPARC	p, 30 GeV	10^{21} pot	visible	(4)	running
proposed						
BDX [130]	JLAB	e^-, 11 GeV	$\sim 10^{22}$ eot/year	recoil e	(1,3)	2024-2025
CODEX-b [131]	CERN	pp, 14 TeV	300 fb^{-1}	visible	(1,2,3,4)	2042
Dark MESA [132]	Mainz	e^-, 155 MeV	150 μA	visible	(1)	< 2030
FACET [133]	CERN	pp, 14 TeV	3 ab^{-1}	visible	(1,2,3,4)	2042
FASER2 [134]	CERN	pp, 14 TeV	3 ab^{-1}	visible	(1,2,3,4)	2042
FLaRE [134]	CERN	pp, 14 TeV	3 ab^{-1}	visible, recoil	(1)	2042
FORMOSA [134]	CERN	pp, 14 TeV	3 ab^{-1}	visible	(1)	2042
Gamma Factory [135]	CERN	photons	up to 10^{25} γ/year	visible	(1,3)	2035-2038?
LBND (DUNE) [136]	FNAL	p, 120 GeV	$\sim 10^{21}$ pot	recoil e, N	(1,2,3,4)	< 2040
LDMX [137]	SLAC	e^-, 4,8 GeV	$2 \cdot 10^{16}$ eot	$\not{p}$, visible	(1)	< 2030
M^3 [138]	FNAL	μ, 15 GeV	10^{10} (10^{13}) mot	$\not{p}$	(1)	proposed
MATHUSLA [139]	CERN	pp, 14 TeV	3 ab^{-1}	visible	(1,2,3,4)	2042
milliQan [140]	CERN	pp, 14 TeV	0.3-3 ab^{-1}	visible	(1)	< 2032
MoeDAL/MAPP [141]	CERN	pp, 14 TeV	30 fb^{-1}	visible	(4)	< 2032
Mu3e [142]	PSI	29 MeV	$10^8 \rightarrow 10^{10}\mu$/s	visible	(1)	< 2038?
NA64$_\mu$ [143]	CERN	μ, 160 GeV	up to 2×10^{13} mot	$\not{p}$	(1)	< 2032
PIONEER [144]	PSI	55-70 MeV, π^+	$0.3 \cdot 10^6 \pi$/s	visible	(4)	approved
SBND [145]	FNAL	p, 8 GeV	$6 \cdot 10^{20}$ pot	recoil Ar	(1)	< 2030

Table A.1: List of past, current and future experiments with their respective FIP sensitivities. The different portals are numbered from 1 to 4 where 1 is the vectorportal, 2 is the scalar portal, 3 is the pseudo-scalar portal and 4 is the fermion(neutrino) portal. Table taken from [4]

Portal	Coupling
(1) Vector: Dark Photon, A'	$-\frac{\varepsilon}{2\cos\theta_W}F'_{\mu\nu}B^{\mu\nu}$
(2) Scalar: Dark Higgs, S	$(\mu S + \lambda_{\mathrm{HS}}S^2)H^\dagger H$
(3) Pseudo-scalar: Axion, a	$\frac{a}{f_a}F_{\mu\nu}\tilde{F}^{\mu\nu}$, $\frac{a}{f_a}G_{i,\mu\nu}\tilde{G}_i^{\mu\nu}$, $\frac{\partial_\mu a}{f_a}\overline{\psi}\gamma^\mu\gamma^5\psi$
(4) Fermion: Heavy Neutral Lepton, N	$y_N LHN$

Table A.2: Coupling Lagrangians for the 4 discussed FIP interaction portals. Through these portals FIPs can potentially approach dark sector particles. Table taken from [8].

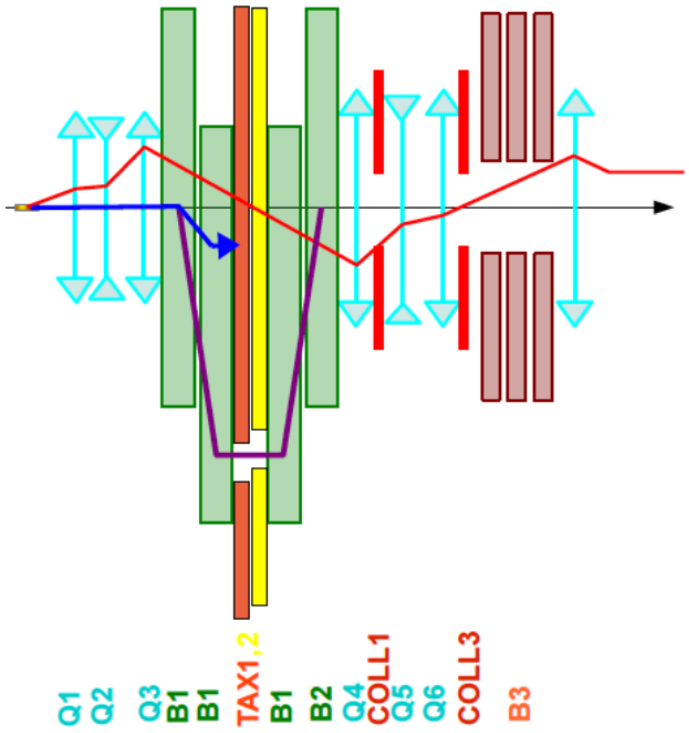

Figure A.1: Different beamline components and path of beam in the different beam dump modes. The purple line shows the path of the kaons and the blue line symbolizes the protons path. Q stands for Quadrupoles, B for bending dipole magnets and COLL for collimators. The red line is related to the beam transport matrix element. Graphic taken from Ref.[4].

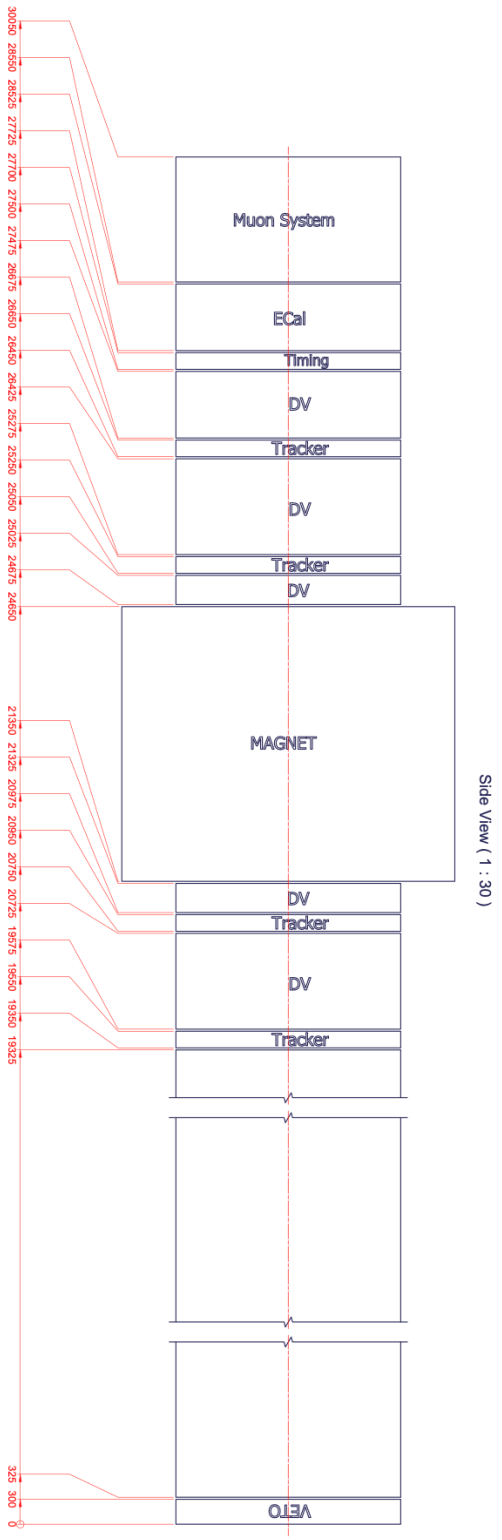

Figure A.2: Exact detector dimensions in mm. The start of the decay vessel is located at 38,5 m, the zero point in the grafic corresponds to 38175 mm in z-direction when choosing the origin at (0,-23.05, 23070) mm. Graphic taken from Ref.[4].

Appendix B

Independence of selection criteria

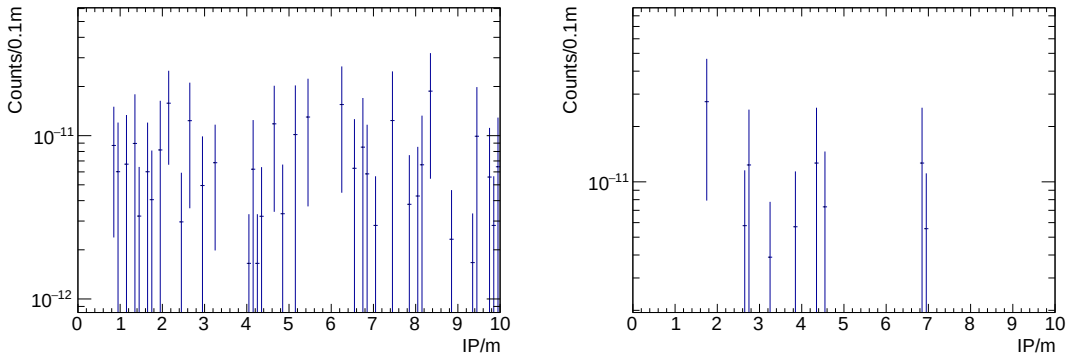

Figure B.1: In the left figure the IPs for particles with momenta between 0 and 0.5 GeV and production points inside of the decay vessel are shown. In the figure on the right the IPs for particle momenta larger than 2 GeV can be seen. A clear relation between momentum and IPs can not be observed.

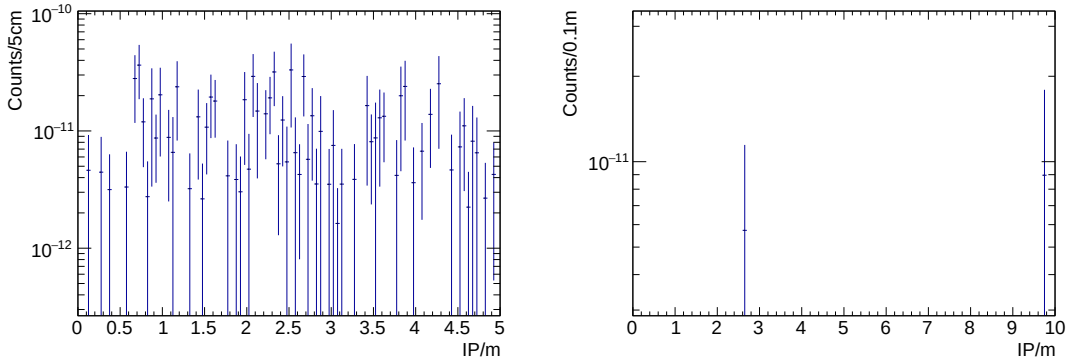

Figure B.2: IPs before and after applying the tracking requirement. The production points for which the IPs are determined are demanded to be located in the decay vessel. A clear dependency cannot be observed but the amount of IPs is too low in the right figure to make a good comparison.

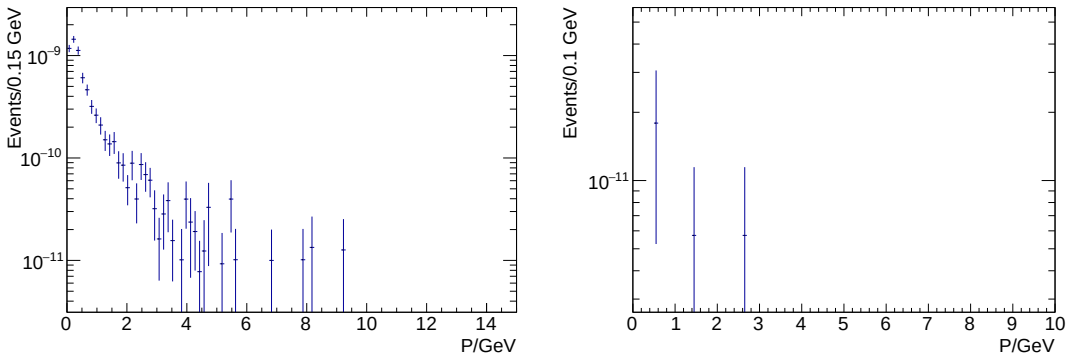

Figure B.3: Momentum before and after applying the tracking requirement, for particles with production points inside of the decay vessel. No clear dependency can be observed.

From observing Figures B.1,B.2 and B.3, there seems to be no clear dependence between the three selection criteria. There might still be a dependence, that can hardly be observed with this amount of statistics. However, since the determination of the total background is just a rough assessment of the upper limit of expected events, a small dependence between the selection criteria could be neglected.

List of Figures

List of Tables

List of Abbreviations

ALP = Axion Like Particle

ASIC = Application-Specific Integrated Circuit

CERN = European Organization for Nuclear Research

DM = Dark Matter

ECAL = Electromagnetic Calorimeter

FIP = Feebly-Interacting Particle

HIKE = High Intensity Kaon Experiments

HNL = Heavy Neutral Lepton

LHC = Large Hadron Collider

MC = Monte Carlo

MIB = Magnetized Iron Block

POT = Protons On Target

PS = Proton Synchrotron

PSB = Proton Synchrotron Booster

SHADOWS = Search For Hidden And Dark Objects With the SPS

SiPM = Silicon Photo Multiplier

SM = Standard Model

SPS = Super Proton Synchrotron

SPSC = SPS Comitee

TAX = Target Attenuator for Experimental areas

WLS = Wave-Length Shifting

Bibliography

[1] J. J. Thomson. “Carriers of negative electricity”. In: *Nobel Lecture, December* 11.1906 (1906), pp. 1901–1921.

[2] L. Meitner and O. R. Frisch. “Disintegration of Uranium by Neutrons: a New Type of Nuclear Reaction”. In: *Nature* (1939). DOI: https://doi.org/10.1038/143239a0.

[3] N. Bohr and J. A. Wheeler. “The Mechanism of Nuclear Fission”. In: *Phys. Rev.* 56 (5 Sept. 1939), pp. 426–450. DOI: 10.1103/PhysRev.56.426.

[4] M. Alviggi et al. *SHADOWS Technical Proposal*. Tech. rep. Geneva: CERN, 2023. URL: https://cds.cern.ch/record/2878470.

[5] M. Thomson. *Modern Particle Physics*. Cambridge University Press, 2013. URL: http://dx.doi.org/10.1017/CBO9781139525367.

[6] Cush. “Standard model of elementary particles”. In: (Nov. 2023). URL: https://en.wikipedia.org/wiki/File:Standard_Model_of_Elementary_Particles.svg.

[7] J. D. Lykken. *Beyond the Standard Model*. 2011. arXiv: 1005.1676 [hep-ph].

[8] G. Lanfranchi, M. Pospelov, and P. Schuster. “The Search for Feebly Interacting Particles”. In: (Sept. 2021). DOI: 10.1146/annurev-nucl-102419-055056.

[9] S. Alekhin et al. “A facility to search for hidden particles at the CERN SPS: the SHiP physics case”. In: *Reports on Progress in Physics* (2016). URL: https://doi.org/10.1088%2F0034-4885%2F79%2F12%2F124201.

[10] B. Batell, M. Pospelov, and A. Ritz. “Exploring portals to a hidden sector through fixed targets”. In: *Physical Review D* (2009). URL: https://doi.org/10.1103%2Fphysrevd.80.095024.

[11] B. Holdom. “Two U(1)’s and charge shifts”. In: *Physics Letters B* 166.2 (1986), pp. 196–198. DOI: https://doi.org/10.1016/0370-2693(86)91377-8.

[12] T. Yanagida. “Horizontal gauge symmetry and masses of neutrinos”. In: *Conf. Proc. C* 7902131 (1979). Ed. by Osamu Sawada and Akio Sugamoto, pp. 95–99.

[13] J. R. Fry. “CP violation and the standard model”. In: *Reports on Progress in Physics* 63.2 (Feb. 2000), p. 117. DOI: 10.1088/0034-4885/63/2/202.

[14] R. Hayano et al. “Antiprotonic helium and CPT invariance”. In: *Reports on Progress in Physics* 70 (Nov. 2007), p. 1995. DOI: 10.1088/0034-4885/70/12/R01.

[15] M. U. Ashraf et al. *High Intensity Kaon Experiments (HIKE) at the CERN SPS: Proposal for Phases 1 and 2*. Tech. rep. Geneva: CERN, 2023. arXiv: 2311.08231. URL: https://cds.cern.ch/record/2878543.

[16] E. Montbarbon et al. “Studies of the conventional beams working group within the physics beyond colliders framework at CERN”. In: *Nuclear Instruments and Methods in Physics Research Section B: Beam Interactions with Materials and Atoms* 464 (2020), pp. 1–4. DOI: https://doi.org/10.1016/j.nimb.2019.11.030.

[17] N. Lurkin. “NA62 framework webpage”. In: (Nov. 2023). URL: https://na62-sw.web.cern.ch/.

[18] C. Bierlich et al. *A comprehensive guide to the physics and usage of PYTHIA 8.3*. 2022. arXiv: 2203.11601 [hep-ph].

[19] I Agapov et al. “BDSIM: Beamline simulation toolkit based on GEANT4”. In: *Tenth European Particle Accelerator Conference" EPAC'06"*. Joint Accelerator Conferences Website. 2006, pp. 2212–2214.

[20] C. Andreopoulos et al. “The GENIE neutrino Monte Carlo generator”. In: *Nuclear Instruments and Methods in Physics Research* 614.1 (2010), pp. 87–104. DOI: https://doi.org/10.1016/j.nima.2009.12.009.

[21] M. H. MacGregor. “Elementary particle lifetimes: An untapped goldmine of information”. In: *The Nature of the Elementary Particle* (1978), pp. 125–149.

Acknowledgements

In the end i want to thank all of the persons who helped me with my work in the last month, this includes understanding physical concepts as well as the proofreading of this thesis.

I want to thank Rainer Stamen for overseeing my analysis, discussing the next steps that had to be done and helping me understand the plots that i generated.

A special thanks goes to Shreya Roy for staying patient with me despite asking many questions and providing me with the signal samples to be able to analyse the ALP signal.

I also want to thank Prof. Schultz–Coulon for supervising this thesis and giving me the opportunity to work on such a interesting project.

Then, i would like to thank Prof. Gastaldo for agreeing to be the second examiner for my bachelors exam.

Many thanks go Moritz who proofread this thesis. Also he was always a few weeks ahead in schedule and always helped me when i had questions.

Thanks to Tobias for proofreading and helping me with questions concerning ROOT or LATEX.

At last i want to thank Gaia and Stefano from the SHADOWS collaboration who always took the time too answer my questions.

Erklärung

Ich versichere, dass ich diese Arbeit selbstständig verfasst und keine anderen als die angegebenen Quellen und Hilfsmittel benutzt habe.

Heidelberg, den 28 November 2023